JPRS-CST-93-002
27 January 1993

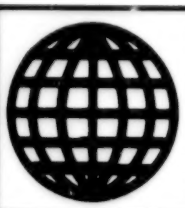

FOREIGN
BROADCAST
INFORMATION
SERVICE

JPRS Report

Science & Technology

China

Science & Technology
China

JPRS-CST-93-002 27 January 1993

CONTENTS

FACTORY AUTOMATION, ROBOTICS

LASERS, SENSORS, OPTICS

MICROELECTRONICS

SUPERCONDUCTIVITY

TELECOMMUNICATIONS R&D

Radar Signal Processing Key State Laboratory Established

93P60102A Beijing ZHONGGUO DIANZI BAO [CHINA ELECTRONICS NEWS] in Chinese 30 Nov 92 p 1

[Article by Xiao Ma [5618 7456]: "Radar Signal Processing Key State Laboratory Established"]

[Summary] A Radar Signal Processing Key State Laboratory, directed by Prof. Wu Shunjun [0702 7311 0689], was formally established at Xidian University in Xian on 20 November. This new facility, one of the first six pilot laboratories to be built by the National Defense Science, Technology and Industry Commission during the Eighth 5-Year Plan, has a gross investment of 13.60 million yuan. So that construction might begin as soon as possible, university officials contributed their own funds even before the State allocation was distributed.

Xi'an High, New-Tech Development Zone Update

93FE0173B Xian SHAANXI RIBAO in Chinese 20 Oct 92 p 6

[Excerpts] [Passage omitted] Xian's high, new-tech development zone is located in the science and education city in the southern part of Xian. It was established in May of 1988 and was designated by the State Council in March of 1991 as one of 27 national high, new-tech development zones. It has the downtown area to the north, Hanshenzhai military industrial zone to the east, and the electronics city with abundant technological and production processing strength to its west. Its total area is 22.35 square kilometers and spreads over four wards of Beilin, Yanta, Lianhu, and Xincheng.

The development zone is backed by a strong science and technology base. There are 22 colleges and universities in the development zone including Xian Jiaotong University, Northwest Polytechnical University, and Xidian University, 44 research institutes of provincial or ministerial level, more than 200 major laboratories including 13 national key laboratories, and has first-class experimental and testing facilities in China. The development zone has a technical staff of 46,700, including 4,384 senior personnel and produces more than 100 national research results annually, and almost 1,000 inventions and patents so far. It is among the top in terms of intelligence and technology concentration.

The development zone benefits from a strong industrial base and a full complement of municipal facilities. There are more than 20 large and medium enterprises in the zone, covering a wide variety of technology including precision machining, optoelectric facility, remote control and remote sensing communication, chemical engineering, precision aerospace machining; many of them are of the advanced international level. The electronics city, an early starter, has completed 70 percent of its construction and has acquired research, development, and production capability. The north border of the development zone is adjacent to the Yihuan Road of the city. The planned Erhuan Road will pass right through the zone and connect it with Xian's transportation system. The communication branch office and wireless station to be built in the zone will make it very convenient.

Preferential policy and brand new management systems are big drivers for the zone. The executive organization of the development zone is the Development Zone Management Committee. The Xian Municipal People's Government has bestowed upon the committee economic management rights. The management committee has the right to decide on foreign investment projects up to US$10 million and domestic investment projects up to 30 million yuan. In the centralized new construction area the committee has the right of a province in making land use decisions. In the policy area the committee has the right of a city in making land use decisions. The committee may process administrative procedures directly. The various municipal committees, offices, and bureaus in principle do not re-examine cases processed by the development zone, but only add their stamps of approval. Based on service requirements and the principle of simplifying administration and improving service, the development zone management committee has a capable management team divided into nine departments. The average age of the workers is 35 and among the 68 workers hired by the committee there are 11 with doctoral or masters' degrees and 90 percent are college graduates. This young and vigorous team is planning the development zone. In addition, supporting service departments such as commerce, tax, financial, customs, export, accounting, business, actuary, legal, and state property management offices all maintain offices in the development zone so that business can be taken care of in a one-stop and efficient manner. System reform is underway for labor, social security, enterprise property rights, finance and accounting, and monetary systems in the development zone. An enterprise entering the zone will operate under these new reformed systems.

Rapid capital construction is a guarantee for the zone's success. Construction in the centralized 3.2 square kilometers of new construction area is progressing rapidly since groundbreaking. To date 1,140 mu of land have been set aside for the area and 206 million yuan were invested for construction. Under construction are 24 plant buildings and associated facilities, covering an area of 280,000 square meters. The first four plant buildings are already completed. Before the end of the year, 11 plant buildings will be finished and 10 companies will move into the new construction zone. [passage omitted] At the end of the year, 440,000 square meters of area will be under construction in the centralized new construction area. The whole area is busy building.

High and new-tech enterprises entering the zone and the numerous high level projects are the base of the development zone. The constantly improving investment environment is attractive to investors here and abroad.

As of the end of August, the number of technology development businesses has increased from 254 in August 1991 to 478. This represents an increase of 88.19 percent, which exceeded the goal of adding 100 companies in 1 year. Foreign investment is on the rise, and the development zone has been visited by 300 groups of investors from 20 countries and regions. As of the end of September 1992, 71 foreign investment businesses were approved, with a total investment of US$97.44 million, 49.3013 million of which was invested by foreign companies. One hundred forty-four enterprises have been approved to move into the centralized new construction area to start 203 projects. The total investment for these projects is 1.17 billion yuan. The anticipated value of production is 3.765 billion yuan, and the tax revenue will be 828 million yuan. These projects will form the backbone industries of electronic information technology, optoelectronic and mechanical integration, high efficiency energy conservation, biotechnology and medicine, and new materials. By the end of this century, the Xian development zone will have a total income of 6 billion yuan from technology, industry, and trade, and will generate 1.2 billion yuan of tax revenue. The total value of industrial production of the development zone will go from 1 percent of Xian's total value of industrial production in 1991 to 10 percent at the end of the century. [passage omitted]

Preferential Policy for Xi'an High, New-Tech Development Zone

93FE0173C Xian SHAANXI RIBAO in Chinese 20 Oct 92 p 6

[Text] The state has allowed the Xian high and new-tech development zone to have preferential policies equivalent to those in coastal economic zones. The Xian municipal people's government has announced parallel preferential policies in 16 areas, giving the development zone projects the same rights as the city in economic management. The incentives are mainly in the following areas.

I. Taxes

The income tax of new and high-tech businesses which started with foreign investment and have operated for more than 10 years will be waived for 3 years starting the first year of profit making. In the fourth to sixth years such businesses will be taxed at one-half of 15 percent.

The income tax of new and high-tech businesses which started with domestic investments will be waived for 3 years starting the first month of sales. From the fourth year to the sixth year, the income tax will be collected at one-half of 15 percent. After the tax reduction period, the businesses will be taxed at 15 percent of sales. Enterprises where the value of exported products exceeds 50 percent of its gross value of production in that year will be taxed at 10 percent of sales. City realty tax and vehicle and boat license fees will be waived for enterprises with foreign investment. City tax and site occupation fee will be waived for land used by foreign investment enterprises. High and new-tech enterprises in the development zone will not be subjected to bonus tax, and the starting level for personal income adjustment tax is 600 yuan per month.

II. Imports, Exports and Tariffs

Bonded warehouses and bonded factories may be set up in the development zone. Export products from processing imported raw materials and parts shall be exempted from import tax, tax for the imported products and tax on the added value of the products. Raw materials and parts imported for the purpose of producing export products shall be exempted from import license. Export products, except those restricted by the state, shall be exempted from export duties. Imported meters, instruments, and equipment unavailable in China shall be exempted from import duties, tax on the imported products, tax on the added value, and uniform industrial commercial tax.

III. Depreciation

High and new-tech enterprises and foreign investment enterprises may accelerate the depreciation of their fixed assets, with approval, over a period of 4 to 7 years.

IV. Finance

Enterprises of foreign investment, when unable to balance the foreign exchange, may buy foreign exchange on the foreign currency adjustment market or from other enterprises. With approval, the enterprise may be given preference to export products produced locally in order to increase foreign exchange. The planning department of the local municipality may allocate a certain amount of foreign exchange. Enterprises producing products to replace imports, with approval, may demand foreign exchange for part or all of its products sold on the Chinese market. Foreign financial institutions may establish branch offices in the development zone. The enterprises may open more than one account. The enterprises and the banks may practice two-way selection. The banks shall give enterprises in the development zone preferential loans and interest rates. With approval, enterprises which invested in the development zone may issue bonds and stocks.

V. Personnel

Documents for personnel from the development zone to go overseas shall be valid for 3 years once they are approved. Foreign investors who have invested more than US$250,000 at one time may be approved to have a certain number of city residence permits for their dependents. Investors from outside the area who invested more than 2 million yuan may be approved for a certain number of city residence permits.

VI. Other

All legal income obtained by foreign enterprise may be freely transferred out of China. The broker who brought in the foreign investment shall be given a commission of 0.5 to 2 percent of the total amount of investment.

The high and new-tech enterprises may set their own prices for their products.

Foreign exchange earned by enterprises in the development zone shall be retained by the enterprises for the first 3 years. Fifty percent of the exchange shall be retained as cash and the other 50 percent retained in a rated way. From the fourth year onward, the percentage retained in cash remains the same, but the portion retained in rated way shall be divided by the local government and the enterprise on a 40:60 percent basis.

Chinatron Corporation Builds High-Tech Electronics Park in Yantai

93FE0173A Beijing ZHONGGUO DIANZI BAO [CHINA ELECTRONICS NEWS] in Chinese 30 Oct 92 p 1

[Article by Tai Chirong [6733 2170 2837] and Zhang Dafang [1728 1129 2397]]

[Text] On 18 October, amid the popping of firecrackers, the high-tech electronics park in Yantai development zone held a ceremony to lay its foundation.

This modern high-tech electronics park combines electronics technology research and production, living and entertainment, and leisure and vacation. It is being built by Kexin New Technology Development Company, which was started with the joint investment by the China Information Trust Investment Company (under Chinatron Corporation) and the Yantai Development Zone Electronics Industry Company. The park includes almost 200,000 square meters of electronics industry zone, 100,000 square meters of public facility zone and 100,000 square meters of residential zone, plus several tens of thousands of square meters of beach front vacation homes. Kexin Company plans to spend 3 years to establish an electronics industrial system based on new technologies but coexisting with high-tech and traditional technology. The company will combine outside financing, internal resources and self-development of the park. The electronics park plans to have development and production in electronic information technology, mechanical and electronic integration technology, new electronics material technology, bioengineering technology and other high and new technologies. The first phase of construction will be completed in the third quarter of 1993.

Officials of the China Information Trust Investment Company said that all those investing in businesses in the park will be eligible for the double preferential policy of the Yantai development zone and the new high-tech development zone. They also qualify for the following five preferences regarding plant building, residence, vacation home, and model selection: (1) investors in the first phase have priority, (2) high-tech projects have priority, (3) high efficiency projects have priority, (4) export projects creating foreign exchange have priority, and (5) projects with large-scale economy have priority. The electronics park allows joint investment and technical cooperation by Chinese and foreign investors, investments solely by foreign investors, businesses started by Chinese enterprises including sole investors, joint investment or technical cooperation, and businesses may also be started by joint investment or cooperation with Kexin Company. Investors may purchase or rent general plant buildings in the park.

CAS Life Organic Chemistry Laboratory in Shanghai

93FE0144A Beijing HUAXUE TONGBAO [CHEMISTRY] in Chinese No 8, Aug 92 pp 49-50

[Article by Yang Binghui [2799 3521 6540] of the Shanghai Institute of Organic Chemistry, Chinese Academy of Sciences]

[Text] In 1985 the Shanghai Institute of Organic Chemistry of the Chinese Academy of Sciences considered organizing a new laboratory in their existing fields of bio-organic chemistry and natural product chemistry to track leading research in the international arena. In 1988, an expert group led by Professor Xing Qiyi [6717 0366 3015] deliberated and passed the establishment of a national priority laboratory, to be named the Life Organic Chemistry Laboratory. After 3 years of work, the laboratory was finished and certified by the state in December 1991.

The laboratory followed the principle of "open, united, and dynamic" and has the objectives of strengthening leading edge basic research in life organic chemistry, forming and cultivating a high level research team, advocating and encouraging interdisciplinary activity, promoting academic and personnel exchange here and abroad, and striving for high standard research results.

I. Research Direction and Content

The Life Organic Chemistry Laboratory mainly engages in frontier research in biological organic chemistry and natural product chemistry. The main research tools are organic structural analysis, organic synthesis, and physical organic chemistry. The objects of study are organic compounds vital for physiological functions in the life process. The laboratory started research on the relationship between structure, synthesis and functions for the dynamic process in biological bodies. These compounds were artificially produced with organic synthesis. New similar compounds were also simulated and their role in the life process investigated. On a molecular basis, further understanding of the life phenomena and the processes they participate in and control has been obtained. This research has opened new avenues for the advancement of life science, human health, and application of agricultural production.

In the short term, the major research contents are:

1. Methodology for Physiologically Active Material Research

This includes the study of chemical methodology of active molecules in organisms. The points of emphasis are the separation of trace, unstable biological molecules,

structural evaluation, and the research of spatial selective synthesis of complex molecules.

2. Chemical Information Molecules

This includes the separation of new chemical information molecules that transmit chemical information between entities, between cells, and within cells. It also includes the determination of their structure, the chemical synthesis method, and the information transmission mechanism of the molecules.

3. Biological Catalyst Systems

This includes the reconstruction and modification of natural enzyme, including ribozyme, with chemical and biological methods and to study the structure-function relationship. The goal is to obtain organic compounds superior to natural enzyme in some respects, to design and synthesize haptene, and to induce the generation and selection of antigen with superior catalytic properties for studying the organic reaction of certain catalytic processes.

4. Oligosaccharide Chemistry

This involves structural determination for oligosaccharide and its conjugates and the study of their chemical synthesis, the synthesis, structure and function relationship of highly physiologically active oligosaccharide, and the separation, purification and structure-function relationship study of intrinsically active polysaccharide and saccharide conjugates.

II. Laboratory Facility and Research Resources

To build the Life Organic Chemistry Laboratory, the state invested 7.1 million yuan, the Chinese Academy of Sciences invested 820,000 yuan, the host unit Shanghai Institute of Organic Chemistry provided eight sets of equipment at a cost of 654,000 yuan. The remodeled 1,000 square-meter laboratory has a brand new look. The major equipment includes NMR spectrometer (AMX-600), gas chromatograph and liquid chromatograph (GC/LC), mass spectrometer and VG Quattro, fluorescent spectrophotometer (LS-50), and ultraviolet spectrophotometer (HP 8451A), a polarization spectrophotometer (241 MC), a circular dichroism dispersion spectrometer (J500), a gas chromatograph (SP 6000), a high pressure liquid chromatograph (LKB-200, HP1090M), and other instruments.

Large instruments of the Shanghai Institute of Organic Chemistry, such as high resolution mass spectrometer, Fourier transformation infrared spectrometer, ferromagnetic resonance spectrometer, photoelectron energy spectrometer, nuclear magnetic resonance spectrometer, trace element analysis laboratory and computer systems have also provided convenience for the cooperation. These facilities helped the laboratory to assume national key projects, to open to the outside, and to host visiting scientists.

The AMX-600 superconducting NMR spectrometer is China's first commercial NMR spectrometer with the highest magnetic field. In addition to multi-nuclei, multi-channel, multi-pulse, and multi-quanta features, the spectrometer also has reversal technology, selective excitation technology, three-dimensional spectrum technology, and "spin-locking" technology; it may be used to perform HOHAHA experiments. The VG Quattro is a new triple quadrupole mass spectrometer with a measurement range up to 4,000 amu. It has capillary GC/MS combination, common EI/CI source, FAB source, LC/MS dynamic FAB sampling probe, and can be used in combination with LC. These instruments are powerful tools for studying the layered structure of complex organic compounds and trace natural products.

The director of the academic committee of the laboratory is Huang Weiyuan [7806 4850 0997], member of the Academic Council of the Chinese Academy of Sciences. Deputy directors are Professor Zhang Lihe [1728 4409 0735], and scientists Wu Yulin [0702 3022 2651] and Wang Yahui [3769 0068 6540]. The laboratory director is Wu Yulin. Wu is a 1962 graduate of the Jilin University chemistry department, a 1966 graduate of the Shanghai Institute of Organic Chemistry and a student of Professor Huang Minglong [7806 7686 7893]. From 1980 to 1982 he was a postdoctoral visiting scholar of Syntex in the United States. His research has earned National Invention Award and Natural Science Award of the Chinese Academy of Sciences.

The laboratory has 33 permanent staff, including 25 researchers. The researchers include four Ph.D. advisors, 13 M.S. advisors and eight full-time technical staff in charge of instrument maintenance and testing. In the 3 years since the laboratory was established, it has trained 63 graduate students; seven of them have graduated with Ph.D., 18 with M.S. and one with a postdoctoral degree.

III. Research Results and Open Laboratory

The Shanghai Institute of Organic Chemistry has over 30 years of history in material chemistry research related to life processes. Under the leadership of the late Director Zhuang Changgong [8369 7022 1872], late Professor Huang Minglong, and Professor Wang You [3076 3731], who is still active at the frontline of research, a number of high quality research results have been obtained in the last decades, especially in the last 10 years. The institute received 21 national level awards, 18 awards in the academy, municipal, and ministerial level, and published 180 papers in major journals here and abroad from 1983 to 1987. A research team of which the backbone is middle-aged researchers, but combining three generations, has been formed. The Life Organic Chemistry Laboratory was established on this basis, which gave the laboratory a head start.

In 3 years the laboratory has formed 13 research groups and obtained encouraging results. The modified sharpless epoxide reagent and its application in synthesis has earned a third natural science award from the Chinese

Academy of Sciences. The structural determination and synthesis of insectile pheromone earned a third prize for S&T advancement from the Chinese Academy of Sciences. The utilization of swine deoxycholic acid was given a third level award by Shanghai Municipality. Microbial triple oil recovery achieved by biological surface activity research passed the assessment, in October 1990, a major result in the national Seventh 5-Year Plan priority projects. Total synthesis of natural lupinidine for anti-malaria purposes marked another advance in China's organic synthesis capability. In the last 3 years the laboratory has published 131 research papers and presented 76 papers in academic meetings, received two patents, published one book in Chinese and passed seven research result certifications.

The laboratory has been open to the outside for more than a year and has approved two open foundations. Currently there are 27 research projects, with 14 of them (51.9 percent) conducted outside the laboratory. The projects are making normal progress and some of them have begun publishing papers. In this period, the laboratory has hosted 24 visiting scientists for a total of 44 man-visits. The research staff in national priority laboratories are floating; we shall adopt an elimination system for the research projects and a floating system for the permanent staff. We enthusiastically welcome colleagues here and abroad to come to the laboratory and study biological organic chemistry.

New Drug Research Laboratory Profiled

93FE0144B Beijing HUAXUE TONGBAO [CHEMISTRY] in Chinese No 8, Aug 92 pp 51-52

[Article by Xie Yuyuan [6200 3022 0337] of the Shanghai Institute of Materia Medica, Chinese Academy of Sciences]

[Text]

I. Introduction to the Laboratory

Based on objective needs and available resources, the Shanghai Institute of Materia Medica began to establish a national key laboratory, the New Drug Research Laboratory, in 1987 to develop new drugs and to train personnel. After discussion by the expert group of the Chinese Academy of Sciences and the State Planning Commission, and site visit by the World Bank, it was approved to be a national key laboratory to be built with a loan from the World Bank and was designated as one of seven testing point laboratories. The laboratory was opened to the outside in October 1990. In April 1991 the first academic committee was formed and the first group of visiting scholar research topics were approved.

The personnel of the laboratory consists of a permanent staff (including four researchers and six associate researchers) and visiting staff up to 50 (there are 10 at this time). The disciplines involved include the major topics for new drug research such as plant chemistry, organic synthesis, biochemistry, biochemical pharmacology, quantum pharmacology, pharmacology, toxicology, and others. Currently there are 10 Ph.D. and M.S. graduate students and one postdoctor. The laboratory director is Xie Yuyuan, and the deputy directors are Li Zhiyi [2621 1807 3015], Qian Peili [6929 5563 7787], and Hu Guoyuan [5170 0948 3220]. The chairman of the academic committee is Gu Zhiping [7357 5347 5493] and the vice chairman is Fang Qicheng [2455 6386 4453].

The laboratory is under the jurisdiction of the Shanghai Institute of Materia Medica of the Chinese Academy of Sciences. It is located in the main courtyard of the Shanghai branch of the Chinese Academy of Sciences where the environment is pleasant and the location is close to many research institutes. It is next to the Shanghai Institute of Biochemistry, Institute of Cell Biology, Institute of Physiology, and the Institute for Brain Research. Opportunities for cooperation abound and the Shanghai S&T Information Center of the Academy provides library information services. Departments in the Shanghai Institute of Materia Medica are able to provide any necessary supporting technology. Currently available major instruments include high resolution mass spectrometer, 400 MHz NMR spectrometer, infrared, ultraviolet, and circular dichroism instrument, and electron microscope. These instruments are powerful tools for research. Logistic services provide excellent research and living environment for visitors. Equipment to be bought with World Bank loans will further improve the laboratory facility.

II. Research Direction and Major Projects

New drug research is a composite discipline resulting from the interaction of chemistry and biology. The need for new drugs prompted the development in other fields, which in turn provided new avenues for new drug research. New drug research is an endeavor that benefits human society and has considerable social and economic payoff. With the development of various new drugs, many diseases such as bacteria infection and tuberculosis are no longer a threat. But some diseases such as tumors, cardiovascular disease, and the recently spreading AIDS still go unchecked and threaten human life. With time there will be other new epidemics requiring new special drugs.

China has a superior natural environment and rich biological resources, plus a long history of traditional medicine and remedies. Our laboratory combined traditional Chinese herbal medicine and the newest theory and technique and focused on China's unique biological resources to search for new drugs for tumors, cardiovascular diseases, and major disorders of the nerve system. The laboratory currently has the following research topics:

1. Separation, Purification, Determination of Chemical Structure, and Synthesis of Active Materials

Physiologically active natural materials have had a long history of study both in China and overseas. The special structure and unique activity of the materials have long held the interest of people. However, the active ingredients

of natural materials are often available only in trace amounts and the structures are often very complicated. For example the concentration of the cancer fighting maytansine in the maytan tree is only one part in 10 million. Through the purification, structural determination, and synthesis of trace active ingredients with complicated structure, not only can new drugs be discovered but natural organic chemistry can also be developed. Traditional Chinese herbal medicine is the most important biological resource. The emphasis should be on the discovery of less-studied botanical resources, especially those in remote border regions of China. New drugs effective for common diseases such as tumors and cardiovascular disease or for regulating the immune system should be developed. In the meantime, traces of active materials, such as active peptide, should be extracted from animal organs and their physiological functions investigated.

2. Selection of New Drugs

The main task of pharmacologists in the study of new drugs is to discover compounds with physiological activity and then optimize them into drugs with certain medical cure. New compounds with curing or prevention functions can reflect their special function only through appropriate screening model. In our laboratory we shall gradually change the traditional whole-body animal model used in the screening of new drugs. Beginning from the theories of enzymes and receptors, we shall establish various sensitive and highly specialized extracorporeal experimental models. For example, we hope to overcome the difficulties encountered by traditional methods due to the trace quantity and specific action of biological active materials in natural products by using cell culture, receptor combination, and enzyme activity experiments. This should improve the screening efficiency and the probability of discovering new drugs.

3. Extracorporeal Toxicity Test for New Drugs

Extracorporeal toxicity tests have unique advantages, including small consumption of material, short test cycle, and rigorous control. For this reason, they play a special role in the development of new drugs. Extracorporeal tests can quickly provide toxicity information and allow the comparison of a series of compounds. They can help the screening of new drugs and problem evaluation of drugs already in the clinical test stage. Quick extracorporeal experiments can continually provide toxicity information of new drugs under study for determining the next steps. On the other hand, based on animal test data and the target organ identified to be reacting to the toxicity, culture of the target cell may be used for in-depth study of the toxicity mechanism and the interaction between the drug and the biological macromolecule. By interpreting the mechanism of the drug action and the toxicity mechanism, a basis may be formed for the molecular design of drugs from a biochemistry point of view.

4. Computer-Assisted Pharmacological Molecular Design, Structure Modification, and Mechanism Study

Quantum pharmacology and computer-assisted molecular design for drugs are becoming increasingly active in pharmacological chemistry and modern pharmacology research. By studying the internal biological process of a newly discovered active material and using quantum chemistry calculation and computer graphics, drugs may be designed and their structure and mechanism studied.

In our laboratory we use methods of quantum chemistry and molecular mechanics in the study of the action mechanism of drugs from a molecular and electronic level. Examples of study are the location of the activity and drug effect picture, the selectivity of the drug-receptor combination, the electronic structure of the drug-receptor complex, and its hydrophobicity. Through this theoretical research, a school of thought and theoretical basis will be formed for the structural modification, molecular design, and molecular pharmacology of natural and synthetic active materials. In this approach a new avenue for searching for new drugs will be gradually established. This new approach will combine theoretical research and experimental investigation and will combine theory, molecular design, synthesis and pharmacological studies into a whole process.

III. Laboratory Policy and Management System

The laboratory operates under a system of "united, dynamic and open" policy. Under the leadership of the host Shanghai Institute of Drug Research, we seek to strengthen our cooperation with other domestic and foreign research and production institutes. We enthusiastically welcome Chinese and foreign scientists working on related research to come as visiting professors and scholars. All those interested may ask for an application form from the laboratory and send it in with a resume and two letters of recommendation. Invitation procedures will ensue with the consent of the laboratory academic committee. Visiting scientists with their research topics may also apply by providing details to the laboratory. The research topics will be evaluated by the academic committee.

We wish to work together with our domestic and foreign colleagues so that the laboratory may combine chemistry and biology, and experiment and theory. We hope to form an applied basic research system to deal with the early phase issues, from the discovery of precursor compound, to the mechanism relationship study, to molecular design for the drug, to synthesis and to toxicity tests. We would like to continue the search for new drugs and the training of researchers so that our laboratory may become an important base in China's new drug research.

Spaceflight Development Strategy; Medium, Long-Term Program for S&T Development

93FE0236A Beijing ZHONGGUO KEJI LUNTAN [FORUM ON SCIENCE AND TECHNOLOGY IN CHINA] in Chinese No 6, Nov 1992 pp 9-12

[Article edited by Zhang Wanbin [1728 5502 2430]: "Nation's Spaceflight Development Strategy; Mid-, Long-Term S&T Program"]

[Text] Over the past three decades, under the policy of self-reliance, hard work and cooperation, China's aerospace industry has followed a path of development that is unique to the Chinese culture; its accomplishments are recognized around the world. Specifically, China has developed a comprehensive aerospace system including research, production, and launch facilities, telemetry and control, and applications; it has established detailed operating procedures, guidelines, rules and regulations; it has cultivated a team of highly qualified and highly motivated aerospace engineers and scientists; and it has developed and successfully launched 25 military and commercial satellites. In the area of providing carrier service on recoverable satellites and launch service on one of its launch vehicles, China is now in a good position to compete on the world market.

China's aerospace industry has developed under very poor industrial and economic conditions; therefore, although it has developed a few state-of-the-art technologies, there still exist many weak spots. From the system point of view, China's aerospace technology is lacking in depth and breadth; in the areas of product quality, operating life and reliability, China is still far behind many developed countries, particularly in space electronics technology. In the area of application satellites, the number of product types is inadequate to meet the needs of national defense and economic development; the satellite technology is rather unsophisticated, its operating life is short and its reliability is rather poor. Also, because of the lack of technical coordination, the capabilities of satellites already in orbit are not fully utilized. In the area of launch vehicles, the payload capability is low, and the use of strap-on technology for heavy launch vehicles is still in its infant stage. In the area of launch systems, improvements need to be made in automation, system layout, orbit determination, and data transmission; also, we need to develop manned spaceflight technology, which is currently in the conceptual development stage. In short, China's aerospace industry is facing the challenges of rapidly advancing technology on the one hand, and the tremendous pressure of domestic needs on the other. In order to ensure that China's aerospace industry will continue to grow, it is essential to maintain the current momentum of space-technology development, and to establish strategies and guidelines for future S&T development.

I. Development Strategies and Targets

1. Development Strategies

Our main strategy is to focus on key technical issues, to improve efficiency and coordination, and to achieve breakthroughs in certain important areas in order to close the gap with advanced nations. Priority must be given to the effort of establishing an independent research and production system, and to basic research and technological reforms. It is important to pursue a policy of uniform development in different areas, and to apply the fruits of aerospace research as much as possible. Significant resources should be devoted to building multi-payload launch vehicles, multi-function satellites, multi-purpose ground stations and multi-station sites. It is also important to establish a serialized, generalized and standardized system for our products, and to intensify our efforts in international cooperation and develop international markets.

2. S&T Targets for Year 2000

These are: (1) to develop additional application satellites with higher performance, improved reliability and longer life; (2) to promote satellite applications such as earth resources observation, communications and broadcasting, navigation and positioning; (3) to derive better economic, military and social benefits from S&T research programs; (4) to achieve breakthroughs in manned spaceflight technology with the goal of sending astronauts into space on Chinese-built space vehicles; and (5) to lay the foundation for building a space station for the next century. In the area of basic research, the goals would be to build integrated research and test facilities for developing advanced aerospace products; to initiate reforms in traditional technical and management procedures using modern technologies; to promote digital and computer control techniques, computer-aided design, manufacturing and management techniques, and experiment with flexible manufacturing procedures; to establish aerospace standards, regulations and manuals which are consistent with the Chinese culture and at the same time satisfy the needs of the international markets; and to develop competitive non-aerospace products and aerospace-related commercial technologies.

3. S&T Targets for Year 2020

These are: (1) to continue developing different types of application satellites and ground systems, and to raise their technical standards to world levels; (2) to use low-cost, non-toxic and high-energy propellants for the nation's family of launch vehicles; (3) to complete the development of a semi-reusable space shuttle system and a manned spaceflight system; and (4) to build new bases for recovering launch vehicles and for tracking and controlling satellites in order to meet the needs of economic development, national defense and space research. In the area of basic research, priority must be

given to constructing well-equipped, complete test facilities for space research and mastering the key technologies in order to lay the foundation for China to become a semi-developed country by the middle of the 21st Century. In industrial production, it is important to promote the use of computers for unified design, manufacturing, test and management, and implement integrated automation systems.

II. Priority Tasks and Key Technologies

1. Priority Tasks

Before the year 2000, four types of application satellites: communications/broadcasting satellites, meteorological satellites, earth resource satellites and military surveillance and mapping satellites are expected to be in routine service; the utility of these satellites will be extended to the areas of navigation and positioning, tracking and data relay, mobile communication, disaster relief, and to the study of microgravity, biology, solar and geophysics and astronomy. Before 2020, continuing efforts will be devoted to improving the performance and efficiency of the satellites already in operation, and to improving the product line of the application satellite system. In the area of launch vehicles, a family of small and medium launch vehicles will be developed before the year 2000; such launch vehicles will be able to deliver an 8-ton payload into a low-earth orbit or a 4.5-ton payload into geosynchronous-transfer orbit. Heavy launch vehicles powered by high-energy, low-cost and non-toxic propellants and space shuttle systems will also be developed. The heavy launch vehicles and space shuttle systems are expected to become operational by 2020. In the area of launch systems, before the next century, Jiuquan, Taiyuan and Xichang will continue to serve as China's basic launch centers; new launch facilities that can accommodate second-generation launch vehicles, geosynchronous satellites and polar-orbit satellites will be constructed; technical zones and launch/recovery zones for manned space vehicles will also be built. By 2020, construction of these zones will be completed. In the area of tracking and control systems, C-band and S-band tracking and control networks and integrated data communication networks are expected to be established before the next century. By 2020, tracking and data-relay satellite systems will be developed, and permanent command centers for manned space missions will be constructed. In the area of satellite applications, efforts will be accelerated to apply satellite technologies to communications and broadcasting, disaster monitoring, agriculture and forestry, oceanography, mapping, finance, transportation, national security, education and space science. Before 2020, priority will be given to establishing China's satellite communications network, a national satellite information center for monitoring and predicting natural disasters, a national satellite resource remote-sensing center and integrated test site, as well as integrated satellite application systems for national security and space science. In the area of manned space stations, development of experimental manned space vehicles and launch vehicles as well as related technologies such as scientific application of microgravity, launch and tracking/control systems, and space medicine are expected to be completed before the end of this century. Manned space vehicles will first be flight-tested without carrying passengers; the tested space vehicles will be used to send China's astronauts into space. By 2020, an experimental space station will be built; future development of the space station is expected to provide economic, military and social benefits. It is of particular importance that processing and production techniques of space materials be developed.

2. Key Technologies

In the area of propulsion technology, priority will be given to research and development of low-cost, non-toxic, high-thrust hydrocarbon engines, large hydrogen-oxygen engines, high-performance orbit-transfer engines, ion engines, high-energy solid propellants, and space-shuttle propulsion systems. In the area of special satellite technologies, efforts will be devoted to the study of high-precision ultraviolet, infrared, visible-light, CCD, microwave remote-sensing and processing techniques; high-efficiency onboard power supplies; light-weight deployable solar arrays, large antenna arrays, antenna beam-shaping and thermal control techniques; modular cabin structures; and onboard payloads which include K, S and L-band equipment and transponders, as well as payloads for studying microgravity, biology, solar and geophysics and astronomy. In the area of tracking and control technologies, efforts will be devoted to the study of large-capacity, high-speed data transmission, satellite data relay, satellite-to-ground and satellite-to-satellite acquisition and tracking, and multiple-target tracking and monitoring, precision orbit determination, miniaturization of sensors and onboard equipment, and adaptive, computer-controlled telemetry. In the area of satellite application technologies, priority will be given to the development of digital communications, mobile communications, techniques for receiving, processing, interpreting and utilizing remote sensing data, as well as navigation and positioning and mapping techniques. In the area of launch and recovery technologies, priority will be given to the development of automated systems for testing and inspecting launch vehicles and space vehicles, automated command, control and communication systems, vertical testing and smoke-exhaust management techniques, large parachutes, as well as recovery and safety processing, cooling, cleaning, emergency and rescue procedures. In the area of manned spaceflight technologies, efforts will be devoted to the development of spacecraft control and life-preservation systems, as well as procedures for emergency and rescue control, reentry and recovery, selecting and training astronauts, providing medical care, medical support and nutrition, and protective measures against environmental effects; efforts will also be devoted to the research and development of on-orbit operations such as space rendezvous, docking, supply, assembly, maintenance and repair, and the construction of long-life, high-power energy supply

systems, ground simulation training facilities and equipment, and experimental facilities for space medicine and other space-station applications.

3. General Technologies

In the area of computer technology and applications, efforts will be devoted to the development of high-precision, high-speed, high-reliability, long-life special-purpose onboard computers which are small and light-weight, and have real-time capabilities. Efforts will also be devoted to the study of new technologies such as radiation hardening, electromagnetic compatibility, leakage prevention, distributed and parallel processing, fault tolerance and artificial intelligence, and to the application of computer-aided design, manufacturing and testing. In the area of special-purpose electronic components, priority will be given to achieving breakthroughs in very-large-scale (VLSI), very-high-speed (VHSIC) and microwave integrated circuit technologies to meet space requirements; significant efforts will be devoted to the development of VLSIs and real-time processing VHSICs, application-specific hybrid integrated circuits, microwave components and high-speed electronic components, and the establishment of unified system design standards. In the area of new materials, priority will be given to the development of high-malleability, high-strength, high-rigidity and light-weight alloys, metal and ceramic-based and carbon-carbon composite materials, special engineering plastics, special-function and multi-function materials, as well as high-energy propellants; efforts will also be devoted to the study of aluminum-lithium alloys and single-crystal materials to be used for high-temperature (1,350°K) turbine blades, and to the study of super single-crystal materials, directional crystals, high-temperature ceramics to further improve the temperature-resistant property of turbine materials to 1,600°K. In the area of new processing technologies, priority will be given to the development of such techniques as ultra-precision processing, special processing, plastic shaping, diffusion welding, wire-net printing, flexible manufacturing and high-energy beam processing; efforts will also be devoted to the use of distributed engineering data management systems and intelligent application software, and to the promotion of unified computer-aided design, computer-aided manufacturing and flexible manufacturing techniques. In the area of basic technologies, it is essential to apply advanced techniques and construct the necessary data bases for space research activities including information gathering, standardization, document filing and inventory.

III. Support Conditions and Major Efforts

1. Providing Unified Leadership and Establishing Rules and Regulations

To develop China's aerospace industry, it is necessary for the Party Central Committee, the State Council and the Central Military Commission to provide unified leadership and overall planning, and to establish guidelines and policies. Specifically, management procedures and rules and regulations concerning the application and approval of funds, management of funds, management of import and export activities, as well as on-orbit management and utilization of application satellites must be clearly established.

2. Establishing Research and Development System and Management Organization

The existing research, design and manufacturing facilities must be strengthened and improved, and research efforts in space microelectronics and satellite applications must be increased. It is also important to coordinate the development of China's aviation industry and aerospace industry in order to exchange new technologies between the two industries.

3. Continuing Efforts To Cultivate Future Scientists and Engineers

By 1995, key members of the current aerospace team will have reached retirement age; therefore, it is important to emphasize the continuing education and health maintenance for today's middle-aged scientific and engineering personnel and to encourage them to pursue further on-the-job training in both research and production. Policies should be established to preserve the number of technical staff at launch centers, tracking and control stations, and research and production facilities, and to prevent draining of technical personnel to foreign countries.

4. Establishing Limited Goals and Priorities

Aerospace technology is a competitive field where many countries are devoting a considerable amount of their national resources. In order to maintain China's current potential and its position in this international competition, considering China's limited financial resources, it is important to establish a limited set of goals and priorities for our development efforts. Complete commitment should be made to research areas that have been designated as high-priority targets; efforts should also be devoted to tracking the development of state-of-the-art technologies. Basic research programs should be highly focused to provide maximum benefits for meeting specific goals.

5. Exploring Other Investment Sources for the Aerospace Industry

Currently, the primary source of investment for China's aerospace industry is from the State. However, with increasing demand, the research funds allocated by the State can no longer meet the needs of continuing development. During the Seventh 5-Year Plan, an itemized investment policy was implemented; in the future, the State funds must be supplemented by other sources of investment such as user investment, military trade, technology transfer and other commercial business activities.

6. Establishing a Technology Base and Initiating Technical Reform

A key factor that tends to retard the growth of China's aerospace industry is the lack of complementary test facilities. Because of insufficient funds, the research facilities constructed during the 1950's and 1960's cannot be renovated or rebuilt, and the existing launch sites and tracking and control stations cannot keep up with development needs. This is an urgent issue that must be addressed. Specifically, China should have a systematic plan to organize a group of key laboratories at the national level and the ministry level; these would include: a simulation center, microelectronics center, failure analysis center, composite materials research center, aerodynamics research center, space environment laboratory, strength and environment laboratory, electromagnetic compatibility laboratory, space engine test center, and computer-aided design and manufacturing center. In addition, data collection and processing systems should be established and management reform should be instituted in order to develop the full potential of these new facilities.

7. Emphasizing the Importance of Continued Coordination

The development of China's aerospace industry has depended on close coordination among different organizations in this country. Under the new contract-based business system, new regulations and procedures should be established to define the relationships and responsibilities of the State, user organizations, research organizations, and testing organizations. Policies to protect the development of aerospace technologies should be established to ensure close coordination and strict adherence to the overall plan during each stage of development.

8. Promoting International Cooperation and Technical Exchange

Aerospace technology is a politically sensitive high technology which cannot be easily transferred from one country to another through simple cooperation. But with the advancement of aerospace technologies, the degree of difficulty and the large scope of the technical projects require increasing amounts of investment to achieve major breakthroughs in key technologies. This is a difficult task for any one country (even a superpower) to accomplish. Therefore, it would be prudent for China to pursue a strategy of selective international cooperation and technical exchange, while adhering to the policy of self-reliance. Hopefully, this strategy will bring in certain key technologies to benefit China's aerospace industry.

9. Insisting on Military and Civilian Cooperation in Our Overall Planning Strategy

Our overall goal is to coordinate China's aerospace development, with emphasis on both military applications and commercial products. The relationships between political considerations and economic and social benefits must be clearly understood and carefully managed. Special efforts should be made to transfer aerospace technologies to various commercial organizations to fully exploit the secondary benefits of aerospace technologies.

10. Encouraging the Commercialization of Aerospace Technologies

Commercialization of the products of aerospace research will have positive effects in terms of obtaining research funds, increasing industrial productivity and making Chinese products more competitive on the world market. Currently, China is a relatively new player on the international market; it still lags behind other countries in terms of product standards, variety, business management, sales facilities and service quality. However, its products are very competitive in price, reliability, after-sales service and warranty policies; consequently, they are well received by consumers around the world. It is important that we capitalize on our strengths and improve upon our weaknesses in order to maintain and further develop our market share. The introduction of Chinese aerospace products to the international market not only is symbolic of China's military, economic and scientific strength, but also is a key factor in China's balance of trade. Therefore, it is essential that we establish favorable policies and conditions to further encourage China's aerospace manufacturers to compete on the world market.

LM-2D Launch Vehicle Detailed

93FE0171A Beijing ZHONGGUO HANGTIAN [AEROSPACE CHINA] in Chinese
No 10, Oct 92 pp 14-17

[Article by Sun Jingliang [1327 2417 5328], chief designer of LM-2D Launch Vehicle: "Long March 2D Launch Vehicle"]

[Text] Abstract: The LM-2D launch vehicle is a newly developed two-stage rocket which has been used to successfully inject one of China's second-generation recoverable satellites into orbit. In this paper, the system design and system components of this launch vehicle are discussed and the flight test results from its maiden flight are presented.

Introduction

At 1600 Beijing time, 9 August 1992, the Chinese-built Long March-2D launch vehicle made its maiden flight from the Jiuquan Satellite Launch Center, successfully injecting one of China's second-generation recoverable scientific satellites into a predesignated orbit. The flight test was completed satisfactorily.

The LM-2D is a two-stage rocket which uses normal-temperature liquid propellant. Its design is based on the LM-4 three-stage rocket with many desirable features including good performance, good adaptability and low cost.

I. System Design

1. Key Technical Parameters

The overall length of the LM-2D (including the satellite) is 38.311 m; the length of the second stage is 13.414 m and its diameter is 3.35 m. The thrust at lift-off is 2961.6 kN and the lift-off weight is 231.671 tons. The configuration of the launch vehicle is shown in Figure 1 and the key technical parameters are listed in Table 1.

Table 1. Key Technical Parameters of the LM-2D

Parameter	First stage	Second stage	
		Main engine	Vernier engine
Lift-off weight (tons)	231.671	40.690	
Structural weight (kg)	9865	3222	
Length (m)	38.311	13.414	
Diameter (m)	3.35	3.35	
Engine thrust (kN)	2961.6	719.8	46.1
Specific impulse (N-sec/kg)	2550	2822	2762
Engine burn time (sec)	152.676	115.200	144.960

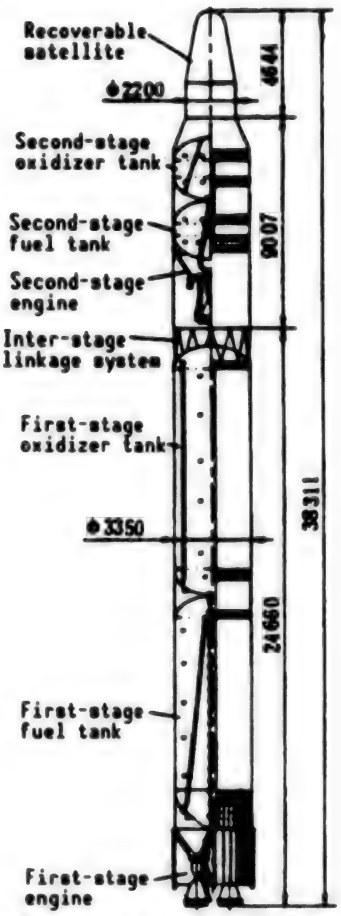

Figure 1. Configuration of the LM-2D Launch Vehicle

2. Payload Capability

A unique feature of the LM-2D is that its first stage has a booster engine and an extended propellant tank. With orbit optimization, its low-orbit payload capability can reach 3300 kg, which greatly exceeds the capability of China's existing two-stage launch vehicles. The calculated payload capability for the LM-2D is shown in Figure 2.

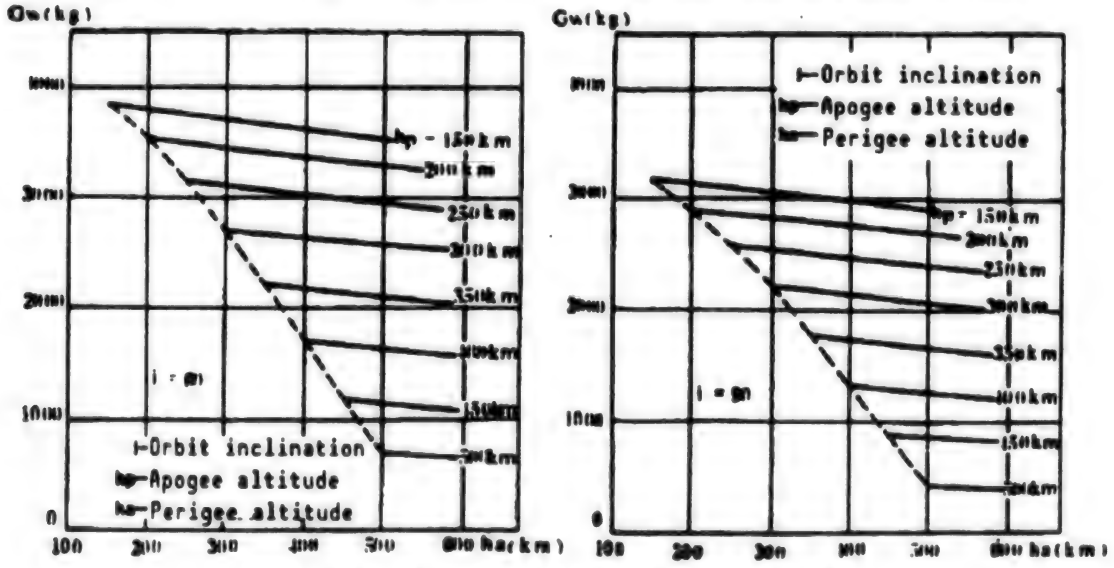

Figure 2. Payload Capability of the LM-2D Launch Vehicle

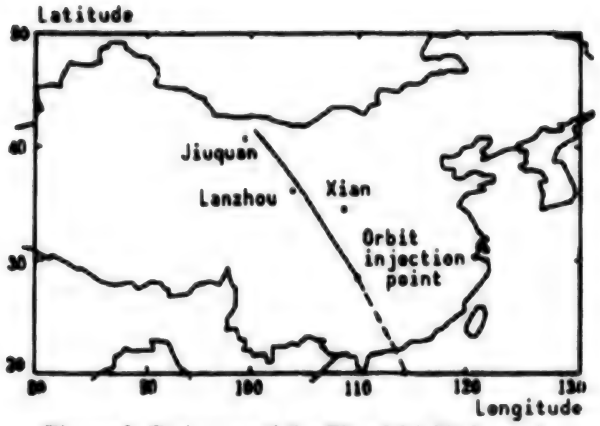

Figure 3. Trajectory of the First LM-2D Launch Vehicle

3. Twelve seconds after lift-off, the launch vehicle executes a preprogrammed turn maneuver and continues on this course for 152.676 seconds when the first-stage engine is shut off; 1.2 seconds later, the first stage is separated. After separation, this stage flies along a ballistic trajectory for 334 seconds before it falls back to Earth; the impact point is in the vicinity of Gangu, approximately 180 km southeast of Lanzhou City. After first and second stage separation, the second- stage engines continue to operate for 115.2 seconds before the main engine is shut off; the vernier engines continue to operate for another 144.96 seconds, at which point they are also shut off. Three seconds after vernier-engine cut-off the satellite is separated from the launch vehicle.

The launch azimuth is 144.4668 degrees. The total flight time between lift-off and separation is 417.036 seconds, and the range is 1674 km; the lift path of the launch vehicle covers six provinces: Inner Mongolia, Gansu, Shaanxi, Sichuan, Hubei and Hunan. Separation of the satellite and the rocket takes place above Jishou City in Hunan Province, and the altitude of separation is 173.6 km. The ground track of the launch vehicle trajectory is shown in Figure 3.

4. Separation Procedure

Separation of the first and second stages of the LM-2D is accomplished using conventional thermal separation techniques; separation of the satellite from the launch vehicle is accomplished using explosive bolts and retrorockets. During separation, the satellite is first unlocked by the explosive bolts, then the two symmetrical retrorockets are simultaneously ignited; one second later, the third retrorocket is ignited, and imparts a 6.1 degrees/second angular velocity to the second-stage rocket. The final separation velocity can reach 0.8 meter/second.

5. Reliability

Table 2 shows a comparison of the reliability estimates of the two LM-4 rockets and the LM-2D rocket.

Table 2. Comparison of the Reliability Estimates of the LM-2D and LM-4

Model	Engine	Pressurized supply system	Control system	Rocket structure	Separation system	Safety system	Overall system reliability
LM-2D	0.9861	0.9937	0.9281	1	0.9858	0.9998	0.9000
LM-4	0.9959	0.9996	0.9300	1	0.9967	0.9999	0.9240

II. System Components

1. Rocket Body

The rocket body consists of the first-stage tail section, the rear transition section, the fuel tank, the inter-tank section, the oxidizer tank, the inter-stage section, and the second-stage fuel tank, the inter-tank section, the oxidizer tank and the instrument compartment. The second-stage instrument compartment is a newly designed riveted structure made of aluminum alloys. The second-stage oxidizer tank and fuel tank are equipped with anti-sloshing plates.

2. Engine System

The first stage consists of four engines connected in parallel; each engine can swivel in the tangential direction, the maximum swivel angle being 10 degrees. The second stage has one main engine and four vernier engines which can also swivel in the tangential direction; the maximum swivel angle is 59 degrees.

3. Pressurized Supply System

Both the first and second stages use a constant-flow-rate auto- pressurization design. During the coast phase of the trajectory, pressurization of the second-stage storage tanks is accomplished by free expansion of the gas inside the tanks in order to meet the intake pressure requirement at the pump of the vernier engines. To suppress the vibration caused by longitudinal coupling between the rocket body and the supply system, the first- and second-stage oxidizer supply lines are equipped with leather-type pressure containers; stability analysis shows that the operating volumes of the containers are 1.2 liters and 0.6 liter, respectively.

4. Control System

The control system consists of the guidance system, the attitude control system, and the timing and command system. Figure 4 shows a block diagram of the onboard instruments of the control system.

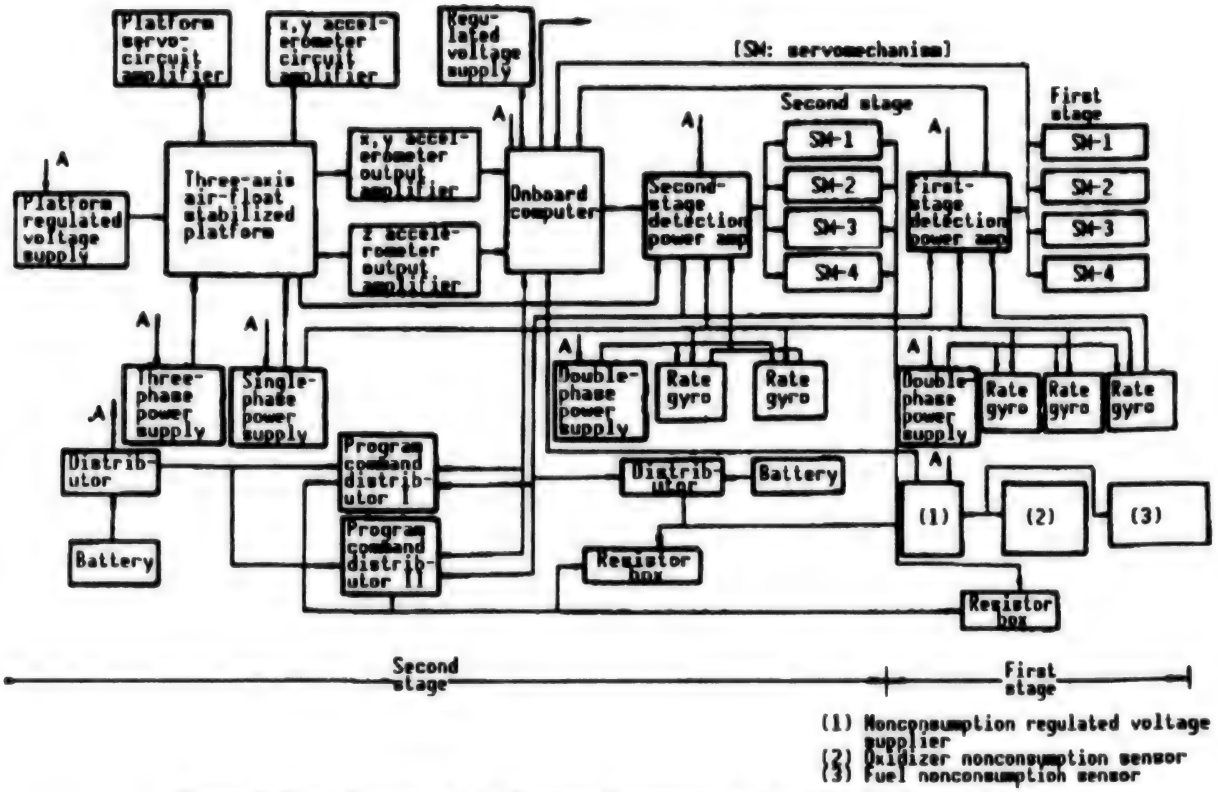

Figure 4. Block Diagram of the Onboard Instruments of the LM-2D Control System

The guidance system uses a platform computer design. In order to achieve the required satellite orbit parameters, the LM-2D launch vehicle must control its orbit to a high degree of accuracy. This is accomplished by optimizing the guidance coefficients and the engine cutoff coefficients.

The attitude control system is a digital system with platform and rate-gyro sensors; it shares the same computer with the guidance system to perform the digital control function.

Because the LM-2D has eliminated the stabilizing tail fins from the original LM-4 design, its first stage is statically unstable, and there is cross coupling between the rigid-body and elastic modes. However,this problem can be solved by choosing a proper location for the rate-gyro and by optimizing the design parameters of the control system via ground simulation tests.

The second-stage pitch and yaw channels use a rate-gyro design and a filter network in place of the conventional differential network; this design has improved the overall system stability, reduced the requirement of dynamic response of the platform damper, and also improved the interference rejection capability of the system.

The timing and command system consists of the onboard computer and two program command distributors. The onboard computer emits drive pulses based on the preprogrammed flight time commands to operate the distributors; the distributors in turn transmit control signals to control the flight sequence of the launch vehicle.

5. Telemetry System

In accordance with telemetry parameter measurement requirements, the telemetry system uses pulse-amplitude-coded FM system large-velocity-variation telemetry equipment, measuring a total of 208 electric and nonelectric parameters. The corresponding sensors and converters all use miniaturized equipment.

6. Range Safety System

The range safety system consists of a continuous-wave (CW) positioning responder, a monopulse coherent responder, a safety command receiver, and the corresponding antennas and controllers. The equipment onboard the launch vehicle shares the same guidance beacon system with the satellite to meet ground tracking requirements.

To improve measurement accuracy, a three-station tracking network is used. This requires redesigning the antenna of the onboard CW Doppler and positioning

transponders to provide a wider beam pattern. As a consequence, tighter requirements are imposed on the antenna performance in terms of polarization, axial ratio, phase characteristics and isolation. Both ground test and flight test results have shown that this system meets the original design specifications.

III. Flight Test Results

The flight test results from 9 August 1992 show that all performance indices of the LM-2D meet design requirements. Some of the key performance parameters are discussed below.

1. Payload Capability. Based on the measured liquid-level readings, the residual oxidizer and fuel in the second-stage storage tanks are respectively 669 kg and 549 kg. Calculations show that after deducting the fuel reserves to meet safety requirements, the actual payload capability is 3329 kg. This is consistent with the predicted results, which illustrates that the approach used for optimum orbit design is valid.

2. Orbit Injection Accuracy. Flight test results show that the accuracy requirements of all six orbit elements of the satellite are satisfied by the launch vehicle (Table 3). This illustrates that in the system design, the optimization approach used by the guidance system with respect to different error sources is quite effective.

Table 3. Deviations in Orbit Elements

Deviation in orbit element	Unit	Design value	Flight test value
Deviation in period	Seconds	+/-6	-2.842
Deviation in inclination	Degrees	+/-0.2	0.08892
Deviation in perigee altitude	km	+/-5	0.126
Deviation in argument of latitude	Degrees	+/-1	-0.20066
Deviation in right ascension of ascending node	Degrees	+/- 0.1	-0.04547
Deviation in argument of perigee	Degrees	+/-5	-2.37387

3. Reliability. While the two flight tests of the LM-4 were successful, there are still two unresolved issues. One is the 8-Hz flutter problem in the roll channel; the other is the fact that in the vicinity of engine cut-off, the interior pressure of the first-stage fuel tank is close to its lower limit.

Ground simulation tests and theoretical analyses have verified that the so-called 8-Hz flutter in the first-stage roll channel is attributable to the presence of a nonlinear link in the closed-loop circuit formed by the rocket and the launch platform; it is a stable, self-excited oscillation induced by the inertial force of the rocking motion of the engine. Once the rocket leaves the launch platform, the flutter phenomenon disappears. Although the flutter amplitude of the servomechanism is only 0.0685 degrees, and the flutter duration is only a little longer than 10 minutes, it nevertheless can have an adverse effect on the engine system. For this reason, a special correction circuit has been designed for the LM-2D attitude control system to suppress self-excited oscillation in the roll channel. During the flight test, the flutter phenomenon between the rocket and the launch platform was absent, which proves that the correction circuit is indeed effective.

A comparison with the LM-4 flight test results shows that the overall pressure increase in the first-stage fuel tank is 0.02-0.03 megapascal below that of the unextended fuel tank, and the pressure level near engine cut-off is close to its lower limit. After analyzing this problem, a decision was made to open the overflow valve of the pressurized supply system to increase the pressure by 0.02 megapascal. Tests show that the lower pressure in the extended fuel tank is caused by losses in the pressurized tube segment between the overflow valve and the storage tank.

IV. Conclusions

The LM-2D two-stage rocket has been developed on the basis of the LM-4 three-stage launch vehicle. Because of its extended first-stage fuel tank and enhanced first-stage engine, it has the largest payload capability among China's two-stage launch vehicles.

By using optimum design techniques in the guidance system, it is possible to achieve orbit-injection accuracy which meets the accuracy requirements of all six orbit elements of the satellite.

In the system design of the LM-2D, reliability improvement measures have been incorporated in certain weak limits of the system; the effectiveness of these measures has been fully demonstrated by flight test results. Therefore, the LM-2D is a high-reliability launch vehicle.

The development cost of the LM-2D is only two-fifths the cost of a single-stage launch vehicle or the cost of one of the older two-stage rockets. In other words, its launch cost per unit payload weight is quite low.

In summary, the LM-2D launch vehicle has many attractive features such as large payload capability, high orbit-injection accuracy, high reliability and low cost.

New Type of Wideband Radar Absorbing Coating Introduced

93P60109A Beijing DIANZI KEXUE XUEKAN [JOURNAL OF ELECTRONICS] in Chinese Vol 14 No 6, Nov 92 pp 618-623

[Article by Feng Lin [7458 2651] and Lu Congxiao [7120 0654 4562] of the Second Department, University of Electronic Science and Technology, Chengdu 610054: "Study of a New Type of Wideband Radar Absorbing Coating," research funded by MAS Institute 621; MS received 21 Aug 91, revised 13 Mar 92]

[Abstract] A new type of wideband composite radar absorbing coating consisting of a band-rejection frequency selective surface (FSS), i.e., a surface constructed of a periodic array of metal-plate resonators, inserted into an ordinary Dallenbach average-loss narrowband coating for metal plates is introduced. This FSS, which completely reflects electromagnetic waves (EMW) in the 2-cm band and completely transmits EMW in the 3-cm band and other bands, provides two absorption peaks in the 8-18 GHz range. For the numerical calculations, electromagnetic parameters $\varepsilon_r' = 10$, $\varepsilon_r'' = 0.3$, $\mu_r' = 1.25$, and $\mu_r'' = 0.75$ (same as for simple Dallenbach coating) are assumed.

Figures 1-4 below show a graph of the reflection coefficient R vs frequency for the simple Dallenbach coating, a schematic of the new composite coating, a diagram of the Jerusalem cross-shaped resonator array, and an equivalent circuit for the composite coating, respectively. Figure 5 below shows a graph of R vs frequency for the composite coating with values w = h = g = 0.1 mm, d = 0.3 mm, p = 4 mm, coating thickness H_1 = 1.5 mm, and coating thickness H_2 = 2.2 mm (curve a) or 2.0 mm (curve b). Figure 6 below shows a graph of R vs frequency for the composite coating with values p = 4.5 mm, H_1 = 1.8 mm, H_2 = 2.0 mm, and w = h = 0.3 mm, d = 0.6 mm (curve a) or w = h = 0.1 mm, d = 0.4 mm (curve b). As can be seen from Figures 5 and 6, absorption peaks are in the -20 dB to -30 dB range.

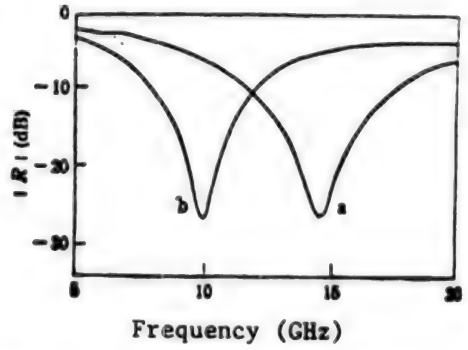

Figure 1. Reflection Coefficient of Simple Coating

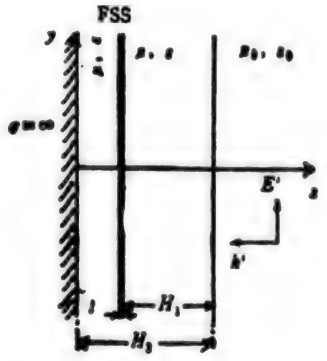

Figure 2. Schematic of Composite Coating Structure

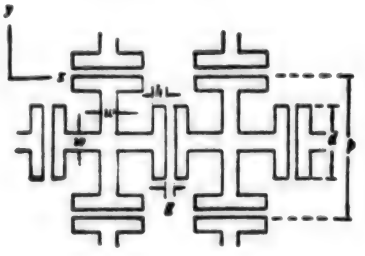

Figure 3. Jerusalem Cross-Shaped Resonator Array

References

1. E. F. Knott et al., "Radar Scattering Cross Section: Estimation, Measurement, and Reduction," trans. Ruan Yingzheng, Chen Hai et al., Electronics Industry Publ. House, Beijing, 1988, Chap. 9.

2. Liu Junneng, YINSHEN JISHU [STEALTH TECHNOLOGY], 1990, No 1, pp 52-68.

3. Zhao Jiasheng, Huang Shangrui, "Electromagnetic Fields and Microwave Techniques," Huazhong (Central China) Univ. of Science & Technology Publ. House, Wuhan, Dec. 1990, Chap. 6.

4. N. Marcuvitz, "Waveguide Handbook," M.I.T. Rad. Lab. Ser., No 10, New York: McGraw-Hill, 1951, Chap. 5, pp 280-292.

5. I. Anderson, BELL SYST. TECH. J., 54 (1975) 10, 1725-1731.

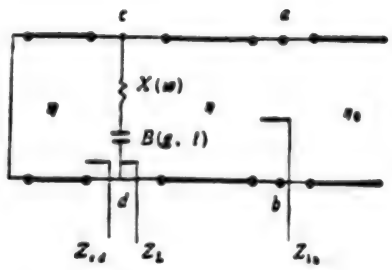

Figure 4. Equivalent Circuit for Composite Coating

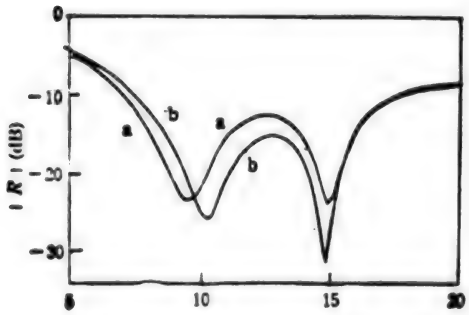

Figure 5. Reflection Coefficient for Composite Coating (value set #1)

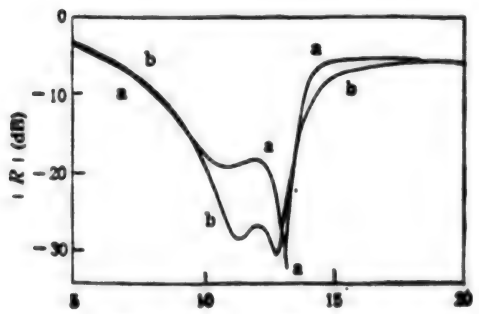

Figure 6. Reflection Coefficient for Composite Coating (value set #2)

Winged Missile Stealth Expert Interviewed

93P60113A Beijing ZHONGGUO KEXUE BAO [CHINESE SCIENCE NEWS] in Chinese
11 Dec 92 p 2

[Article by Yu Keli [0060 0344 6849]: "Visit With Winged Missile Stealth Technology Engineer Zhang Chongxue"]

[Summary] Zhang Chongxue [1728 1504 1331], who in 1987 graduated at 22 from Nanjing Aeronautical Engineering Institute (NAEI), participated in four winged missile [i.e., cruise missiles and other finned aircraft-type missiles] stealth technology research projects from 1989 to 1992, and has been awarded 1st- and 2nd-class S&T advancement medals from MAS. MAS Third Design Institute experts selected him in 1987 from over 100 NAEI graduates in radio technology, at a time when the nation's winged missile stealth technology R&D was just beginning (MAS had no expert in this area at that time). In 1989, young engineer Zhang participated in the NDSTIC Seventh 5-Year Plan key project entitled "Distributional Signatures of Winged Missile Radar Strong Scattering Sources" and also in the project "Study of RCS Algorithms for Analysis of Conventional Winged Missile Scattering Signatures." In July 1992, Engineer Zhang, who has been working closely with colleagues from three different organizations, was given the arduous task of doing the first analysis of scattering characteristics from a live practice experiment, which task is now proceeding quite smoothly. Zhang is currently pursuing graduate studies in the theory and applications of electromagnetic scattering at Beijing Aeronautical Engineering Institute.

Domestic R&D of Fiber Optic Gyros Highlighted

93P60119A Beijing ZHONGGUO HANGTIAN [AEROSPACE CHINA] in Chinese
No 12, Dec 92 pp 28-31

[Article by Zhu Jinmiao [2612 6855 1181] of Shanghai Institute of Precision Instruments (SIPI): "Research, Development of Fiber Optic Gyros"]

[Excerpts] [Passage omitted]

5. Domestic Fiber Optic Gyro (FOG) Research

In the past few years, domestic research on the FOG has begun to move into the applications phase. The measurement accuracy and drift of miniaturized experimental

prototypes are both on the 0.5-1.0°/h level, and measurement range according to the application requirement is 300-600°/s. FOGs capable of measuring higher angular rates are also now in development. Mid-to-low-accuracy FOG research has moved from the laboratory theoretical prototype development phase into the engineering applications research phase. Simultaneously, research on high-accuracy FOGs, completely integrated FOGs, and FOGs based on new principles is also being synchronously conducted.

SIPI began its research on FOGs in 1987. Based on development standards of foreign optical fiber components at that time, a decision was made to concentrate efforts on the all-fiber-type FOG. After several years of effort, promising development achievements have been made. Under laboratory conditions, the main technical indicators of all-fiber FOG prototypes tested are as follows:

threshold $< 1°/h$
drift $< 1°/h$
scale factor stability: better than 10^{-3}
maximum measurable angular rate: 300°/s
exterior dimensions: Φ80 mm x 30 mm

As is evident, the technical indicators of these prototypes have entered the tactical-level gyro category, but it should be noted that these indicators have been obtained only under laboratory conditions. Among three experimental prototypes, the optical fiber coils using polarization-preserving fiber all have fiber lengths of 400 m, and employ 1.3 μm semiconductor devices for the light-emitting sources.

In addition, a miniaturized FOG with equivalent performance has also been developed in the laboratory; in the early engineering scale-up period, the performance drop could not exceed one level of magnitude.

In laboratory simulation, several parameters of the FOG prototypes have been measured, and a severe gyro temperature drift problem was discovered. FOG drift is mainly due to temperature drift. The reasons are as follows: [Passage omitted].

Currrent domestic FOG studies in actuality all revolve around the following four points:

1) Research on raising angular rate measurement sensitivity.
2) Research on expanding measurement range.
3) Research on suppressing drift.
4) Research on preserving FOG performance in the transforming of laboratory prototypes into engineering applications. [passage omitted]

Three-Aircraft Control Simulator Developed by Air Force Institute

93P60107A Beijing KEJI RIBAO [SCIENCE AND TECHNOLOGY DAILY] in Chinese 8 Dec 92 p 1

[Article by Wang Yu [3769 1342] and He Xiquan [6320 6007 3123]: "Chinese Air Force Pioneers Three-Aircraft Control Simulation System"]

[Summary] The three-aircraft simulation system developed over a 6-year period by the Air Force Aeronautical Institute No. 1 passed appraisal a few days ago. This system, according to experts within and outside of the Air Force, is the first in the world to organically fuse the three elements of aerial warfare: the target aircraft, the attack aircraft, and the missile(s); overall technical performance meets early-90s international standards. This conclusion was reached by the China Science and Technology Information Institute, which conducted an online data search of published simulation research in the United States, France, Japan, and the former Soviet Union.

Nation Pioneers New Technology for Fabricating High-Temperature Titanium

93P60114A Beijing RENMIN RIBAO [PEOPLE'S DAILY OVERSEAS EDITION] in Chinese 6 Jan 93 p 1

[Article by Wang Shihuan [3769 0013 3562]: "Nation Pioneers New Technology for Fabricating High-Temperature Titanium"]

[Summary] Xian, 5 Jan (XINHUA)—A 12-year effort to develop an industrial titanium (Ti) alloy capable of withstanding 500°C-plus temperatures has been successfully concluded, with the perfection of a 520°C resistant Ti alloy via a high-temperature deformation toughening technique and the successful application of the new alloy in development of new aircraft types. This achievement, the first of its kind at home or abroad, was realized by engineers from a number of organizations, including Northwest Polytechnical University [in Xian] and the Ministry of Astronautics Industry's Plants 148 and 3007 and Institute 621.

Mechanical Properties of SiC Whisker/Y-TZP (Containing Alumina) Composites

40100048A Beijing GUISUANYAN XUEBAO [JOURNAL OF THE CHINESE CERAMIC SOCIETY] in Chinese Vol 20 No 5, Oct 92 pp 393-397

[English abstract of article by Zhang Yufeng, Guo Jingkun, Huang Xiaoxian, and Li Baoshun, Shanghai Institute of Ceramics, Chinese Academy of Sciences; MS received 25 May 91]

[Text] Effects of SiC whisker content on the mechanical properties of SiC whisker/Y-TZP composites are studied. When SiC whiskers are distributed uniformly in Y-TZP matrix, there is a small amount of monoclinic zirconia in the composites. The transformation of zirconia from tetragonal to monoclinic is the main toughening mechanism. The mechanical properties of the composite are higher than that of the matrix. The composite containing 5% weight alumina possesses excellent mechanical properties. The strength and fracture toughness of the composite containing 5% weight alumina and 20% volume SiC whisker are 1329+/-13 MPa and 14.8+/-0.7 MPa-$m^{1/2}$, respectively. The composites show excellent high-temperature strength and thermal shock resistance.

Mechanical Properties, Microstructure of SiC_w/Mullite, SiC_w/Y-TZP/Mullite Composites

40100048B Beijing GUISUANYAN XUEBAO [JOURNAL OF THE CHINESE CERAMIC SOCIETY] in Chinese Vol 20 No 5, Oct 92 pp 410-416

[English abstract of article by Hong Jinsheng, Huang Xiaoxian, Guo Jingkun, and Li Baoshun, Shanghai Institute of Ceramics, Chinese Academy of Sciences; MS received 14 May 91]

[Text] SiC whisker (SiC_w)/mullite and SiC_w/Y-TZP (yttria-stabilized tetragonal zirconia polycrystal)/mullite composites are fabricated by hot pressing with SiC whiskers and Y-TZP as reinforcing phases. The mechanical properties and microstructure as well as reinforcing mechanisms are investigated. Flexural strength and fracture toughness of mullite are improved by the addition of SiC whiskers. Significant improvement in flexural strength and fracture toughness will be obtained for the SiC_w/Y- TZP/mullite composite, in comparison with the SiC_w/mullite composite. Reinforcing mechanism in the composite is mainly crack deflection induced by SiC whiskers, pullout of SiC whiskers, and microcrack toughening caused by Y-TZP. Interaction of Y-TZP and SiC whiskers has a superposition of coordination effect on the improvement of strength and fracture toughness of mullite.

Oxidation of SiC-Matrix Multiphase Ceramics at High Temperature, Its Effect on Strength

40100048C Beijing GUISUANYAN XUEBAO [JOURNAL OF THE CHINESE CERAMIC SOCIETY] in Chinese Vol 20 No 5, Oct 92 pp 417-423

[English abstract of article by Du Weifang, Xiao Hanning, Du Haiqing, Hunan University; MS received 1 Jun 91]

[Text] The law and the behavior of the oxidation of SiC-matrix multiphase ceramics containing the nonoxide phase of TiC, TiB_2, ZrB_2 and the oxide phase of Al_2O_3, respectively, are studied. Their effect on bending strength of SiC-matrix multiphase ceramics is also studied. The experimental results indicate that the oxidation resistance of SiC-matrix multiphase ceramics containing the nonoxide phase decreases greatly, disastrous rapid oxidation occurs at low temperature, which is related to the kinds of the nonoxide phase and not related to the amounts of the nonoxide phases, and the temperature at which strength decreases is 100-150°C lower than that at which the disastrous oxidation occurs. The oxidation resistance of SiC-matrix multiphase ceramics containing the oxide phase of Al_2O_3 does not change significantly, and the strength at high temperature does not decrease. Degree of oxidation resistance for different SiC-matrix multiphase ceramics is of the following order:

$$SiC\text{-}Al_2O_3 > SiC\text{-}TiC > SiC\text{-}TiB_2 > SiC\text{-}ZrB_2$$

SiC-Whisker Reinforced Al_2O_3-Matrix Composite

40100048D Beijing GUISUANYAN XUEBAO [JOURNAL OF THE CHINESE CERAMIC SOCIETY] in Chinese Vol 20 No 5, Oct 92 pp 424-430

[English abstract of article by Huang Zhengren, Jiang Dongliang, and Tan Shouhong, Shanghai Institute of Ceramics, Chinese Academy of Sciences; MS received 26 Jul 91]

[Text] The mechanical properties of SiC whisker reinforced composite with Al_2O_3-matrix are studied by using different Al_2O_3 powders. Under the optimum processing condition, a flexure strength of σ_f = 780 MPa and a fracture toughness of K_{IC} = 7.6 MPa-$m^{1/2}$ are obtained for Al_2O_3 matrix composite with 30 volume percent SiC whisker. Various dispersion methods are discussed by comparing the homogeneity of whisker dispersions. The influence of whisker dispersion on mechanical properties of composites is studied under various dispersion conditions and a possible toughening mechanism is proposed for whisker agglomerate contribution to toughening. The additional effects of both whisker reinforcement and particle dispersion toughening are also discuss d.

Interfacial Structure, Reaction of Carbon Fiber/Lithium Aluminum Silicate Glass-Ceramic Composites

40100048E Beijing GUISUANYAN XUEBAO [JOURNAL OF THE CHINESE CERAMIC SOCIETY] in Chinese Vol 20 No 5, Oct 92 pp 449-456

[English abstract of article by Wang Xiaoguang, Zhou Ao, et al., Glass Research Institute, China Building Materials Academy; MS received 6 Feb 91]

[Text] Both the interface and the fiber surface in carbon fiber reinforced lithium aluminum silicate glass-ceramic (LAS_I and LAS_{III}) composites hot pressed with different soak time and with different strength and toughness are studied by using, TEM, EDAX, SAD, SEM and XPS, respectively. Hot pressing with a shorter soak time makes the interfacial layer in C fiber-LAS_I thin and relatively compact, while hot pressing with a longer soak time makes the interfacial layer wide and loose. A wide gas diffusion layer as well as NbC grains exist at the interface of C fiber-LAS_{III}. When C fiber-LAS_{III} is hot pressed for a longer soak time, the diffusion layer is thin and NbC deposits on fiber surface; the binding between C fiber and LAS matrix has improved. The interfacial reaction, the interfacial structure formation and their effect on composite properties are discussed.

Properties, Preparation of Composite Ceramics of Al_2O_3/Si_3N_4 of Nano- Submicrometer Size

40100048F Beijing GUISUANYAN XUEBAO [JOURNAL OF THE CHINESE CERAMIC SOCIETY] in Chinese Vol 20 No 5, Oct 92 pp 484-488

[English abstract of article by Zhang Lianmeng, Yu Maoli, et al., Advanced Materials Institute, Wuhan University of Technology; MS received 15 Jul 91]

[Text] Amorphous Si-N ultrafine powder prepared by RF-plasma CVD is converted into Si_3N_4 by heat treatment. The average particle size of the powder is about 0.7 μm. Si_3N_4 and α-Al_2O_3 (average size, 0.5 μm) are used to obtain composites of nano-size dispersoid. The size of scattered phase is 60-120 nm. XRD, SEM, STEM are used to investigate the composite structure and high-temperature performance. Results show that the strength of the composite can be kept up to 1300°C and the transverse bending strength at 1300°C is twice that of Al_2O_3 ceramics.

Neurosurgery Draws World Attention

93FE0145A Beijing LIAOWANG ZHOUKAN [LIAOWANG WEEKLY] in Chinese No 41, 12 Oct 92 pp 36-37

[Article by Liu Jiansheng [0491 1696 3932] and Jiping [4764 1627]]

[Text] Two years ago famous Chinese neurosurgeon Wang Zhongcheng [3769 1813 6134] and his doctoral students first developed an embolic material and applied it to the treatment of craniocerebral angionosis. This development has turned a new page for China's neuroradiology.

Neurosurgery is a young discipline in the realm of medicine in the world. Started from nothing, China has developed its neurosurgery in 40 years. From 1952 and especially in recent years, Chinese neurosurgery has attracted world attention by excelling. China has begun research in neuroepidemiology. The fatality rate of direct surgery for intracranial aneurysm has dropped to below 2 percent. Functional- and spacial-orientation neurosurgery began to develop and advanced microsurgery technologies are being developed and perfected.

Notable Development

Before the People's Republic, China did not have independent neurosurgery: neurosurgery operations were usually done by surgeons. Because of the high degree of difficulty, there were few cases of surgery. The records showed that in the 20 years before 1949, there were only 50 cases of neurosurgery operations performed in Xiehe Hospital in Beijing.

In 1952 pioneers in China's neurosurgery began planning China's own field of neurosurgery. In 1954 Chinese doctors began to study cerebral angiography, a technique of vital importance to neurosurgery. After 10 years of work, angiography was developed and a set of effective diagnostic tools became available. With this pioneering development, the risk of neurosurgery was greatly reduced compared to the old method of pneumoencephalography. After that, China published its first volume on "Cerebral Angiography." Even today, this volume compiled by Dr. Wang Zhongcheng is still of great value. Since then the development of neurosurgery has taken off in China. In the 1950's and 1960's, China was able to treat brain injuries, cranial hematoma, and some brain tumors. In the 1970's, China entered a new age in treating cerebrovascular disease.

Today Chinese neurosurgeons can treat tumors of the central nervous system, cerebrovascular disease, cranial injuries, rachiospinal disorders, epilepsy, and perform spacial-orientation surgery. The quality of surgery for brain stem tumor, cranioaneurysm, cerebral arteriovenous deformation, cranial tumor and craniocerebral trauma has reached the world standard.

Now neurosurgeons are available all over China's major cities and regional hospitals. China has more than 200 neurosurgery centers, 26 neurosurgery research institutes, 10,000 beds and 5,000 to 6,000 neurosurgeons. The high technical standard of the Beijing Institute for Neurosurgery and the Beijing Tiantan Hospital has made them the largest neurosurgery centers in Asia.

Highly Sophisticated Operation

The brain stem is the center for breathing, heart beat, and consciousness. It is called the brain of the brain. Operation on the brain stem has been a forbidden zone for neurosurgeons, but the Chinese doctors have gradually conquered the difficulties of brain stem operations. On 5 March 1991 a 15-year-old patient with central nerve hemiplegia of the left side was diagnosed with CT and magnetic resonance imaging to have brain stem displacement disorder. An operation performed by Professor Wang Zhongcheng, director of the Beijing Neurosurgery Institute and chief neurosurgeon of the Beijing Tiantan Hospital, successfully removed a 2 x 2 x 1 cm tumor from the brain stem bridge. After more than 1 year followup, the examination of July 1992 showed that the brain stem has basically returned to normal. The success of this operation marked a new age for China's neurosurgery. Data shows that in recent years there were 10 cases of brain stem surgery in Beijing's Tiantan Hospital alone.

Statistics show that in developed Western nations cerebrovascular disease is the third major cause of death; in Japan it is the second. In several northern provinces in China, it has become the leading cause of death. For this reason, China pays great attention to the prevention of cerebrovascular disease and the analysis, testing, and control of this disease. In China the direct surgery fatality rate for cranioaneurysm has dropped to below 2 percent and there was a total survival rate for 100 consecutive cranioaneurysm direct surgery. Successful direct surgery has also been achieved for multiple aneurysm and giant aneurysm. In one case the Chinese doctors successfully closed four aneurysms and removed a 9-mm diameter giant non-embolic cystic aneurysm, all in one brain operation. It was a rare case not seen in the world.

Today, the 27 neurosurgery centers in China have all accumulated the experience of treating 1,000 brain tumors. It was estimated that 80,000 cases were treated nationwide. The fatality rate of the operation is about 10 percent and in some centers less than 5 percent. The Beijing Institute for Neurosurgery and Beijing's Tiantan Hospital have treated 76,000 cases of intracranial tumor. In 1991 alone they performed 999 brain tumor operations. The fatality rate has dropped to 2.6 percent, which is the lowest in China.

New Techniques

As technology progresses, Chinese neurosurgeons have introduced and applied CT, magnetic resonance, single-photon emission computer scan, multi-directional ultrasonic Doppler, laser, ultrasonic attraction, surgical

microscope, and vascular embolic materials. These new techniques have raised the diagnostic capability of China's neurosurgery to a new high.

In 1981, there were only eight CT scanners in China, now there are about 400 units. The emergence and application of CT has fundamentally revolutionized the examination and treatment of neurology. It replaced the pneumoencephalography and ventriculography, and reduced the number of cerebral angiography, and is widely used in the examination of neurosurgical diseases.

Magnetic resonance imaging makes use of the signal formed by hydrogen atoms in the body after radio frequency excitation in a magnetic field. It can show certain anatomical physiological changes. It is particularly useful in examining the brain stem, the spine, basal cranial disease, leukoencephal disorder, and other neurosurgical problems.

China has about 10 units of single-photon computerized scanners for neurosurgery. This high-tech instrument is effective for early diagnosis of ischemic cerebrovascular disease, for selecting surgical procedures and evaluating treatment effectiveness, and for verifying origin of epilepsy and diagnosis of Alzheimer's disease. Before the 1970's, there were few surgical microscopes in China. In recent years microsurgery has flourished and become widely used in China. Microsurgery has become a regular part of neurosurgery—about one-third to one-half of neurosurgical operations in China were performed under microscope. Operations for treating cranioaneurysm, cerebral arteriovenous deformation, and for removing tumors from the third ventricle, basal ganglia, thalamus, basis cranii, and brain stem are almost entirely done with microsurgery. Shanghai Huashan Hospital uses microsurgery for removing cerebral arteriovenous deformation with a removal rate of 97 percent and a fatality rate of 0.8 percent. Microsurgery not only has broadened the scope of surgery but also improved the technology and greatly reduced the fatality rate. Microsurgery gave neurosurgery a big jump.

Neuroradiology is a fascinating new field. Intravascular thrombosis examination has been practiced in Beijing, Shanghai, Jiangsu, and Wuhan. The General Hospital of the PLA has applied super-selective, disengagible, saccular catheter technique in treating aneurysm and arteriovenous fistula. The Suzhou Medical School obtained good results in treating arteriovenous aneurysm by injecting isobutyl cyanoacrylate.

Combined with new and high technology, neurosurgery is showing unprecedented vigor in China.

Catching Up on Basic Research

China's neurosurgery started on a weak base and has for a long time lagged behind the world on basic research. But in recent years neurosurgery in China has been more active in basic research. Great strides have been made in neuroepidemiology, cerebrovascular disease, brain tumor, neural medium and the combination of western and Chinese medicine.

In 1981 China surveyed 10,000 residents of western Beijing for nervous system diseases. In 1983 another survey was made among 60,000 residents in six Chinese cities. In 1985, a neuroepidemiological survey was organized in villages of 22 provinces and regions and minority regions to cover 240,000 people. From 1981 to 1985, more than 300,000 people were surveyed. These surveys provided the first batch of valuable data regarding the disease occurrence rate and fatality rate for city and village dwellers of China. These data have received international attention.

Research in functional and space-orientational neurosurgery has advanced neurosurgery one more step toward neurophysiology. Today Chinese medical scientists are exploring world-class problems such as brain transplant technology. Based on traditional Chinese medicine of open skull surgery with acupuncture anesthesia, and the research on blood flow dynamics and neuroendocrinic reaction, the success rate for acupuncture anesthesia open skull operation has reached 90 percent.

In September 1991, the Beijing Institute for Neurosurgery presented a paper on dysfunction of the brain at the Second International Brain Functional Disability Symposium in Italy. The paper received a special honorary mention in the first international research for brain functional disability. This basic research was of the top quality in China or in the world. It enriched the theory of brain dysfunction and provided new clues for the treatment of brain dysfunction.

The rapid advances in neurosurgery in China have attracted international attention. The Neurosurgery Association of the China Medical Society has established an academic exchange relationship with 20 countries and regions. Chinese neurosurgeons have joined the ranks of their advanced world peers with increasingly improved technology.

Large-Scale Culture of Vero Cells in High Density by Using Chinese-Made CellCul-20 Bioreactor

40091005A Beijing SHENGWU GONGCHENG XUEBAO [CHINESE JOURNAL OF BIOTECHNOLOGY] in Chinese Vol 8 No 4, Nov 92 pp 389-393

[English abstract of article by Dong Shupei [5516 2885 3099], Chen Yinliang [7115 0936 5328], et al. of the Research Institute of Biochemical Engineering, East China University of Chemical Technology, Shanghai, Song Jiali [1345 1367 7537], Chen Liesheng [7115 0441 0524], and Chen Wenlan [7115 2429 5695] of Shanghai Institute of Biological Products, Shanghai]

[Text] High density Vero cells were cultivated in a 20 liter CellCul-20 home-made bioreactor and a 2.5 liter

CelliGen. Also, the cell growth, its metabolism and technique of cell transfer and scale-up of culture volume were investigated. GT-2 microcarriers were used and beads to beads transfer technique was employed. It was shown that the efficiency of inoculation was increased and operating steps and risks of contamination were decreased in this experiment. The cell density was higher than 1.0 x 10^7 cells/ml and was 7 times higher in comparing with the inoculation number after 5 days' perfusion cultivation. Obviously, this work is significant for large-scale culture of animal cells in pilot and industrial scales.

Continuous Ethanol Fermentation by Immobilized Cells in External Circulating Fluidized-Bed Reactor at a Pilot Plant Scale

40091005C Beijing SHENGWU GONGCHENG XUEBAO [CHINESE JOURNAL OF BIOTECHNOLOGY] in Chinese Vol 8 No 4, Nov 92 pp 404-406

[English abstract of article by Cheng Linna [4453 3829 1226], Zhu Weixing [2612 4850 0992], et al. of the Institute of Chemical Metallurgy, Academia Sinica, Beijing]

[Text] For this experiment, a superior yeast strain 2201 was selected. The entrapping method of calcium alginate was used. The immobilized cell particles were prepared by the large-scale granulator with a capacity of over 120 L/h. Three-stage series external circulating fluidized-bed reactor with a total effective volume of 665 L has been studied and continuously operated for about 3 months. The experimental results show that when untreated diluted cane molasses containing 15 percent of sugar were used, the final ethanol concentration, the conversion rate to sugar and the reactor productivity were 8-9 percent (v/v) and over 92 percent and 12 kg/m^3-h, respectively, at a feeding rate of 70-110 L/h. The output of ethanol was about 240 L/d.

Key words: External circulating fluidized-bed reactor; immobilized yeast particles; molasses; ethanol

Study on Ferrocene Based Amperometric Sensor for Glutamate Determination

40091005B Beijing SHENGWU GONGCHENG XUEBAO [CHINESE JOURNAL OF BIOTECHNOLOGY] in Chinese Vol 8 No 4, Nov 92 pp 394-400

[English abstract of article by Li Yourong [2621 0645 2837], Chu Ju [0328 3515], and Li Qinshan [2621 7230 1472] of the Research Institute of Biochemical Engineering, East China University of Chemical Technology, Shanghai]

[Text] The study on a new glutamate biosensor, which was mainly composed of glutamate oxidase, ferrocene, graphite and platinum disc was presented. Various factors which influence the response of the biosensor to glutamate and the performance of the electrode were studied. The results show that the optimum pH and temperature for the electrode in CSR [Stirer reaction cell] were 6.8 and 30°C respectively, then in FIA [flow injection analysis] 7.0 and 27°C respectively. Among 25 substrates tested, no apparent response was observed for sugars, organic acids and amino acids, except arginine and alanine. Good linear relationship was obtained within the range of 2.5-25 μl (0.1 mol/L) glutamate. The correlation coefficient of the calibration curve, $r = 0.998$, the response time was 1 min, and the useful life of the sensor was about one week. Satisfactory results were obtained when the biosensor was applied to the determination of glutamate in fermentation process.

Preparation and Utilization of BrdU Antiserum II. Detections of BrdU Labeling Chromosome and DNA Using BrdU Antibody Technique

40091005D Beijing YICHUAN XUEBAO [ACTA GENETICA SINICA] in Chinese Vol 19 No 5, Oct 92 pp 385-389

[English abstract of article by Shang Kegang, Lou Zhuangwei, and Wu Heling of the Department of Biology, Peking University, Beijing 100871]

[Text] Utilizing Chinese-made highly specific BrdU antiserum, via the second antibody being conjugated with enzyme and DAB-H_2O_2 or AEC-H_2O_2 colorific methods, the BrdU marked regions of CHO [ovary of Chinese hamster] and human chromosomes were detected clearly. The BrdU-DNA prints (pg) on nitrocellulose membranes were also showed with similar methods.

Studies of Reform of Yeast Cell by Protoplast Fusion: Genetic Analysis of the Interspecific Fusion Hybrid Between *Saccharomyces cerevisiae* and *S. diastaticus*

40091005E Beijing YICHUAN XUEBAO [ACTA GENETICA SINICA] in Chinese Vol 19 No 5, Oct 92 pp 467-474

[English abstract of article by Li Taosheng [2621 2711 3932], Zhi Huijun [5120 1979 6511], et al. of the Department of Biology, Hangzhou University, Hangzhou. The project supported by the National Natural Science Foundation of China and Zhejiang Provincial Natural Science Foundation of China.]

[Text] The strain HU-KDF-185 tested is an interspecific triploid hybrid obtained by protoplast fusion of a diploid *Saccharomyces cerevisiae* and a haploid *S. diastaticus*. The following aspects were shown in the genetic analysis: (1) The strain HU-KDF-185 was a stable hybrid genetically in terms of the genetic markers. (2) The sporulation rate (i.e., ascus forming rate) of the hybrid was 13.54 percent in general conditions, but it could increase to 38.61 percent in special condition of presporulation culture, and in the case of presporulation culture it also

could reach 33.23 percent even when the hybrid cells were cultured in a simple HU-Li sporulation medium containing only 0.98 percent potassium acetate and 0.186 percent KCl and 2 percent purified agar. 202 asci were dissected and there were only 376 single spore clones, which means that spore viability was about 46.53 percent. (3) The genotype of these spore clones were determined. Mating type of tetrads from the hybrid HU-KDF-185 contained four types: a, α, 2α, and aa, but no aaα mating type. Fermentability of the tetrads for soluble starch was about 1:2 (fermenter: non-fermenter). Genetic markers of the tetrads showed that the prototroph: auxotroph was 1:1.

Key words: Interspecific fused hybrid, *Saccharomyces diastaticus, Genetic analysis*

Construction of a Genomic Library and Cloning of Glucoamylase Gene From *Aspergillus niger*

40091004F Guangzhou ZHONGSHAN DAXUE XUEBAO [ACTA SCIENTIARUM NATURALIUM UNIVERSITATIS SUNYATSENI] in Chinese Vol 31 No 4, Oct 92 pp 86-93

[English abstract of article by Luo Jinxian [5012 6651 6343], Zhang Tianyuan [1728 3240 0337], Li Wenqing [2621 2429 3237], Tan Yuhui [6223 1342 1920], and Wang Yiliang [3769 5030 5328] of the Department of Biology and Biotechnology Research Center; MS received 30 Dec 91]

[Text] A complete genomic library of *Aspergillus niger* was successfully constructed using lambda EMBL3 DNA as vector. The donor *A. niger* DNA was partially cleaved with EcoRI, 15-20 kb fragments were recovered from sucrose gradient and ligated to the vector lambda EMBL3 DNA with T4-DNA ligase at a proper ratio and the ligated mixture was packaged *in vitro* with the packaging extract prepared from E. coli SMR10 single strain system. The packaged phages were titered using *E. coli* 359 as host and 2.5 x 10^5 recombinant phages/ug DNA was obtained, which is 10x more than the number of recombinants required for an entire A. niger genome according to Clarke and Carbon. The glucoamylase gene was screened by *in situ* hybridization. The recombinant plaques were transferred to nitrocellulose filter and hybridize to ^{32}p labelled DNA probe, 2 positive plaques were obtained from 10^5 recombinant phages. After rescreening, DNA was extracted from the positive phage for further analysis. The glucoamylase gene was localized on a 2.5 kb EcoRI-EcoRV fragment by Southern blotting. The 2.5 kb fragment was subcloned in EcoRI site of -EcoRV pBR322.

The Upstream Enhancer Sequence of Yeast Acid Phosphatase Gene PHO5

40091004A Shanghai SHENGWUHUAXUE YU SHENGWUWULI XUEBAO [ACTA BIOCHIMICA ET BIOPHYSICA SINICA] in Chinese Vol 24 No 5, Sep 92 pp 443-449

[English abstract of article by Yan Jun [0917 0193], Yu Qin [2456 0530], and Ao Shizhou [2407 0013 3166] of the National Laboratory of Molecular Biology, Shanghai Institute of Biochemistry, Academia Sinica, 200031]

[Text] The expression of yeast acid phosphatase gene PHO5 is an ideal research system for elucidating the control mechanism of gene transcription.

The PHO5 gene encoding repressible acid phosphatase is transcribed at high levels in media low in inorganic phosphate (Pi). Transcription of the PHO5 gene is repressed when cells are supplied with high Pi in media. The coding region of the PHO5 gene was fused in frame with LacZ and assayed by β-galactosidase activity. Using various restriction endonucleases, the 5'-flanking region of the PHO5 gene was deleted. The levels of gene expression of various deletions show two different functional fragments located at -1386 to -542 and -542 to -273 upstream of the initiation codon, which contain an upstream enhancer sequence (UES) and an upstream activation site (UAS) respectively. PHO5 UES does not promote transcription but it somehow enhances gene expression. To characterize the borders of the PHO5 UES, a number of deletions was studied. The results indicate that PHO5 UES consists of two regions located at -791 to -716 which has 70 percent enhancer power, and at -646 to -585 which has 30 percent power. These two regions have a 27-bp homologous sequence. Transcription of the PHO5 gene is controlled by various DNA elements and they may be associated with different regulatory factors. The molecular mechanism of this regulation involves a complex system of interaction between specific DNA sequences and protein factors.

Site-Directed Mutagenesis of the Major Gene TDH3 Coding for Glyceraldehyde-3-phosphate Dehydrogenase of *Saccharomyces cerevisiae*

40091004B Shanghai SHENGWUHUAXUE YU SHENGWUWULI XUEBAO [ACTA BIOCHIMICA ET BIOPHYSICA SINICA] in Chinese Vol 24 No 5, Sep 92 pp 489-495

[English abstract of article by Wang Enduo [3769 1869 1122], Lu Shennan [7120 6500 2809], and Zhou Guoying [0719 0948 3841] of Shanghai Institute of Biochemistry, Academia Sinica, 200031, Liu Chunrong [0491 2504 2837] of Shanghai Research Center of Biotechnology, Academia Sinica, 200233, and Huang Xiuqin [7806 4423 3830] of the Department of Biology, East China Normal University, Shanghai 200062]

[Text] TDH3, the major gene coding for glyceraldehyde-3-phosphate dehydrogenase of *Saccharomyces cerevisiae* has been cut from pgap491 with restriction endonuclease HindIII and subcloned into M13mp10, to obtain a recombined single-stranded DNA in which the positive strand DNA of M13mp10 is linked to the complementary strand of the TDH3 gene. It was used as a template for the site-directed mutagenesis reaction and two 27 mers ATAAACAAAATGTCGCGAGTTGCTATT [letters TCGC have dots underneath] and AAGCTTGTTTCGCGAGCTTCTTGTACC [letters CGCG have dots

underneath] as primer 1 and primer 2, respectively, after phosphorylation of their 5' terminals, dot marks show the mutation sites. The codons GTTATA for 1-Val and 2-Arg are changed into TCGCGA in primer 1 and TCCAAC for 145-Ser and 146-Asn are changed into TCGCGA in primer 2. Thus the 1-Val and 146-Asn would be changed into 1-Ser and 146-Arg, respectively, and an NruI site is induced in between the two pairs of codons, the first and second residues, 140 and 146 residues. We used Klenow enzyme at 0°C in the mutagenesis reaction. The mutations were screened by digestion of NruI. The efficiency of mutagenesis by primer 1 and primer 2 are 25 percent and 27 percent, respectively, fairly high for a fourbase-change in a 27 mer primer. Uracil-containing ssDNA of mutation 1 derived from *E. coli* RZ1032 was used as a template and primer 2 as a mutagenic primer to carry out the mutagenesis reaction at 0°C with Klenow enzyme. Screening with dot blotting and digestion of NruI, the two-site mutation at an efficiency of 33 percent was obtained. After subcloning of the fragments involved in mutation 1 and mutation 2 into M13, the sequences of mutation 1 and mutation 2 were proved correct.

The Inhibitory Effects of Catechin Derivatives on the Activities of Human Immunodeficiency Virus Reverse Transcriptase and DNA Polymerases

40091004C Beijing ZHONGGUO YIXUE KEXUEYUAN XUEBAO [ACTA ACADEMIAE MEDICINAE SINICAE] in Chinese
Vol 14 No 5, Oct 92 pp 334-338

[English abstract of article by Tao Peizhen [7118 0160 3791], Zhang Tian [4545 1131], et al. of the Institute of Medical Biotechnology, Beijing]

[Text] Catechin derivatives including (-)-epicatechin gallate (ECG), (-)-epigallocatechin gallate (EGCG), (-)-epigallocatechin (EGC) and green tea extract (GTE) were found to inhibit the activities of cloned human immunodeficiency virus type 1 reverse transcriptase (HIV-1 RT), duck hepatitis B virus replication complexes reverse transcriptase (DHBV RCs RT), herpes simplex virus 1 DNA polymerase (HSV-1 DNAP) and cow thymus DNA polymerase α (CT DNAP α). EGCG and ECG were shown to be very potent inhibitors of HIV-1 RT. According to the IC50 values for HIV-1 RT, these compounds can be ordered as EGCG 0.0066 μmol/L > ECG 0.084 μmol/L > GTE 0.1 μg/ml > EGC 7.2 μmol/L. DHBV RCs RT was the least sensitive to these compounds. Kinetic study showed that EGCG exerts a mixed inhibition with respect to external template inducer poly (rA).oligo (dT)12-18 and a noncompetitive inhibition with respect to substrate dTTP for HIV-1 RT. Bovine serum albumin significantly reduced the inhibitory effects of catechin analogues and GTE on HIV-1 RT. In tissue culture GTE inhibited the cytopathic effect of coxsackie B3 virus, but did not inhibit the cytopathic effects of HSV-1, HSV-2, influenza A or influenza B viruses.

Molecular Cytogenetic Study of Short Arm Aberrations in Human D and G Group Chromosomes

40091004D Beijing ZHONGGUO YIXUE KEXUEYUAN XUEBAO [ACTA ACADEMIAE MEDICINAE SINICAE] in Chinese
Vol 14 No 5, Oct 92 pp 339-345

[English abstract of article by Wang Yumei [3769 3768 2734], Cheng Zaiyu [4453 0961 3768], et al. of the Institute of Basic Medical Sciences, Beijing]

[Text] Many structural and functional characteristics in the cen-pter regions of human D and G group chromosomes play important roles in the etiology of genetic diseases and cancer. Six cases of Dp^+/Gp^+, 10 cases of D/G translocation, 1 case of extra small chromosome (mar), and 1 case of Yqs were studied with molecular and cytogenetic techniques. The results showed the Ag-NOR frequency of the Dp^+/Gp^+ group to be significantly higher, but their satellite association frequency lower than those of normal controls. Autoradiographic silver grains were not found along the entire p^+ part of the marker chromosome by using chromosomal *in situ* hybridization techniques. This result is somewhat different from what we had reported previously. It is suggested that the mechanism of p^+ formation may vary among different cases. Diversified nucleolar organizer transcription sites may exist in the rRNA gene cluster region of chromosomes. The results of Ag-NOR and *in situ* hybridization of D/G translocation cases indicate that they have lost their NOR. Study of the extra small chromosome case and the Yqs case suggested that mar and Yqs exert no effect on the phenotype.

Key words: acrocentric chromosome, nucleolar organizer regions (NOR), satellite association (SA), extra small chromosome, chromosomal *in situ* hybridization

Restriction Map and Tc^r Gene Localization of the Truncated Plasmid pAL32 Derived From the Plasmid pCJ3 in *Bacillus pumilus*

40091004E Guangzhou ZHONGSHAN DAXUE XUEBAO [ACTA SCIENTIARUM NATURALIUM UNIVERSITATIS SUNYATSENI] in Chinese
Vol 31 No 4, Oct 92 pp 80-85

[English abstract of article by Zhou Zhenlin [0719 2823 2651], Chen Qi [7115 3823], Wang Ge [3769 7245], and Xu Hong [6079 5725] of the Department of Biology and Biotechnology Research Center]

[Text] The truncated Tc^r plasmid pAL32 derived from the plasmid pCJ3 was cleaved by reciprocal double digestions with 6 restriction endonucleases. The molecular weights of the fragments were estimated by agarose gel electrophoresis. A simple restriction map of pAL32 was thus constructed. Recombinants were obtained by cloning EcoR V fragments of λDNA using Km^rTc^r plasmid pSC33 as vector which was constructed from the plasmid pAL32 and the removed origin plasmid

pUB110. All of them are resistant to Km and sensitive to Tc. A Km^rTc^s recombinant plasmid was also obtained by Pvu II digest from the plasmid pAL32 and pUB110. Based on the inactivation of the tetracycline resistance of these recombinants, it is suggested that EcoR V and Pvu II sites are located on Tc^r gene of the plasmid pAL32.

Key words: tetracycline resistant plasmid, Bacillus pumilus, restriction map, gene localization

Nucleotide Frequency Analysis of Bacteriophage φX174 Genome

40091005F Beijing YICHUAN XUEBAO [ACTA GENETICA SINICA] in Chinese
Vol 19 No 5, Oct 92 pp 475-480

[English abstract of article by Yang Ziheng [2799 1311 1854] of the Department of Animal Science, Beijing Agricultural University; MS received 10 Sep 90]

[Text] Detailed analysis was carried out on the nucleotide frequencies in the genome of bacteriophage φX174. In coding regions the distribution of four nucleotides at the three codon sites was highly non-random, and the patterns were conspicuously similar among the genes, implying that it might be a feature of the genome. An index I_c, which was based on the χ^2 statistics of the site by base 3 x 4 table, was introduced to reveal the extra information embedded in the coding region, and also to discriminate between coding and non-coding open reading frames. Doublet deviation analysis showed that deviation patterns were not significantly related to the codon sites in coding regions, and were also very similar in different genes. Possible mechanisms of such similarity are discussed.

Key words: Bacteriophage φX174, Nucleotide frequencies, Doublet deviation

Molecular Cloning and Identification of 130kd Mosquitocidal Protein Gene of *Bacillus Thuringiensis* Var. *Israelensis* (BTI)

40091005G Beijing WEISHENGWU XUEBAO [ACTA MICROBIOLOGICA SINICA] in Chinese
Vol 32 No 5, 1992 pp 314-319

[English abstract of article by Hua Xuejun [5478 1331 6511] and Fan Yunliu [5400 0061 0362] of Lab. of Molecular Biology, Biotechnology Research Center, Chinese Academy of Agricultural Sciences, Beijing]

[Text] The location of 130kd mosquitocidal protein gene of Bti 4Q5 strain on its 75Md plasmid was confirmed by southern hybridization using an 18-base oligonucleotide probe. The crystal protein containing the component of 130kd toxic protein was purified. The crystal protein exhibiting the mosquitocidal activity against larvae of Aedes aegypti was shown by bioassay. The purified 75Md plasmid DNA of Bti 4Q5 strain was completely digested with HindIII restriction enzyme, ligated with the vector pUC18 and transformed into the recipient cells of *E. coli* TG1. From these transformants, four clones with HindIII restriction fragment inserts highly homologous to the 18-base oligonucleotide probe were obtained by in situ hybridization and southern hybridization. The 5.2kb HindIII restriction fragment insert was obtained in clone pFH2 and clone pFH4, and 2.3kb HindIII restriction fragment insert in clone pFH1 and pFH3. For pFH2 and pFH4, the 5.2kb fragment was inserted in pUC18 in opposite orientation. It contained 130kd mosquitocidal protein gene (type I) identified by restriction enzyme map analysis. The 2.3kb Hind III fragment insert in other two clones (pFH1 and pFH3) harbored a part of the type II mosquitocidal protein gene which can be used as a probe for cloning of the type II mosquitocidal protein gene.

Vibrio Cholerae Toxin B Subunit Gene Expressed in a Salmonella Vaccine Strain

40091005H Beijing WEISHENGWU XUEBAO [ACTA MICROBIOLOGICA SINICA] in Chinese
Vol 32 No 5, 1992 pp 320-327

[English abstract of article by Tian Jinghui [3944 0079 1979] and Lu Deru [7120 1795 1172] of the Second Military Medical University, Shanghai. The project supported by the Health Department of PLA General Logistics.]

[Text] This paper reports that the *V. cholerae* toxin B subunit (ctx B) gene was inserted into pYA 248 plasmid with the aspartate β-semialdehyde dehydrogenase (asd) gene and the recombinant plasmid was transformed into *S. typhimurium* deletting asd gene. Results showed that ctx B gene was highly expressed and secreted into midium. This strain was able to colonize in the intestinal epithelium. Oral immunity and general immunity could produce antibodies at high level and enhance cellular immune responses. The animals orally inoculated with *S. typhimurium* X4072 (pYA-ctx B) vaccine had remarkable protection against virulent *V. cholear* 569B strain and *S. typhimurium* strain. Use of such system provides useful method for vaccine technology.

Key words: *Vibrio cholerae* toxin B subunit gene ctx B; Aspartate β-semialdehyde dehydrogenase (asd); *Salmonella typhimurium*

Regulation of Purine Biosynthesis. I. Isolation of *add*:: MudJ (*lacZ*, Kan^r) Insertions and Genetic Mapping

40091005I Beijing WEISHENGWU XUEBAO [ACTA MICROBIOLOGICA SINICA] in Chinese
Vol 32 No 5, 1992 pp 328-333

[English abstract of article by Wang Aoquan [3769 2407 0356], Chen Xiuzhu [7115 4423 3796], Dai Xiuyu [2071 4423 3768], and Tang Guomin [0781 0948 2404] of the Institute of Microbiology, Academia Sinica, Beijing. Project supported by the National Natural Science Foundation of China.]

[Text] Reported here is the isolation of adenosine deaminase deficient mutants and genetic mapping. Engineering transposon MudJ (*lacZ*, Kan^r) was used for mutagenesis and six *add*:: MudJ were obtained among 20,000 Kan^r transductants. Adenosine deaminase activity of these mutants were assayed and all are negative. Cotransduction analysis of *add*:: MudJ indicated that *add* is 70 percent linked to *pmi*(31') and 37 percent linked to zxx1900::Tn10d-tet insertion which is 10 percent linked to *pur*R(30'). Three points cross showed that add is located between *pmi* and Tn10d-tet insertion. Therefore the gene order is *pur*R-zxx1900::Tn10d-tet-*add-pmi*.

Key words: *Salmonella typhimurium*; Adenosine deaminase deficient mutant; Genetic mapping; Engineering transposon

Isolation and Characterization of Mutactimycin-Producing Mutant

40091005J Beijing WEISHENGWU XUEBAO [ACTA MICROBIOLOGICA SINICA] in Chinese Vol 32 No 5, 1992 pp 353-358

[English abstract of article by Li Huanlou [2621 3562 1236], Lu Wanyu [0712 1238 3842], Zhang Yueqin [1728 2588 3830], et al. of the Institute of Medicinal Biotechnology, Chinese Academy of Medical Sciences, Beijing 100050]

[Text] Natural non-antibiotic producing *Streptomyces* sp. 1254 was mutagenized by UV irradiation and two active mutants were isolated. Mutant 113 produced novel anthracycline compounds designated mutactimycins. Mutactimycin A was active against the bacteriophage of *Bac. subtilis* and some viruses in tissue culture. The mutant 2-6 synthesized a basic water-soluble antimicrobial antibiotic.

Chemical analysis of the whole cell hydrolysate and the morphological characterization showed that the strain 1254 and its mutant 2-6 were of chemotype I, belonging to the genus of *Streptomyces*, and the mutant 113 was of chemotype IV without mycolic acid.

Co-synthesis test of strain 1254 and a blocked mutant of strain 113 gave the active compounds identical with mutactimycins. Using the *act*I gene as a probe, the Southern hybridization revealed homology between the actinorhodin polyketide biosynthase gene and the total DNA of the strain 1254. Based on these data it was deduced that *Streptomyces* sp. 1254 should have a biosynthesis pathway for mutactimycin, but some of its genes might fail in expression and mutagenesis would make the silent gene(s) active.

A New Virus of Rabbit. III. Study on Morphological Superstructure and Antigenicity of Rabbit Hemorrhagic Disease Virus (RHDV)

40091005K Beijing WEISHENGWU XUEBAO [ACTA MICROBIOLOGICA SINICA] in Chinese Vol 32 No 5, 1992 pp 359-363

[English abstract of article by Zhao Lin [6392 2651], Li Tianxian [2621 1131 2009], et al. of the Wuhan Institute of Virology, Academia Sinica, Wuhan 430071]

[Text] In the spring of 1986, an acute infectious disease occurred in Wuhan Second Producing Medical Manufactory, and the rabbit almost completely died. The mortal symptom was tested and the rabbit Hemorrhagic Disease (RHD) was confirmed. RHD epidemic also occurred in Hubei Traditional Chinese Medicine Institute. Having purified viruses of above two sources by low speed, high speed and sucrose density gradient centrifugation, it was found that viruses can react with antiserum of RHDV from Nanjing Agricultural University in agar gel immunodiffusion tests. These results proved that they belong to the same serotype but have different morphological superstructure, viral polypeptides and can't react with antiserum of standard Parvovirus of rabbit. It was concluded that the new RHDV is a new strain.

Construction of the Genomic Library of Cubiodal Polyhedra Mutant of Bombyx Mori Nuclear Polyhedrosis Virus and Isolation of the Polyhedrin Gene

40091005L Beijing WEISHENGWU XUEBAO [ACTA MICROBIOLOGICA SINICA] in Chinese Vol 32 No 5, 1992 pp 376-379

[English abstract of article by Chu Ruiyin [0328 3843 6892], Wang Qinghua [3769 3237 5478], Chen Zhangliang [7115 4545 5328], et al. of the National Laboratory of Protein Engineering and Plant Genetic Engineering, Department of Biology, Beijing University, Beijing]

[Text] A mutant with cubiodal polyhedra which isolated from wild type Bombyx mori nuclear polyhedrosis virus with that of hexagonal polyhedra was used as an experimental material. By using alkali lysis procedure, the viral DNA fragments were cloned into plasmid pBluescript. Five recombinants containing polyhedrin gene were selected through in situ hybridization. The inserted 10.6 Kb fragment was mapped and an additional Xho I site was found upstream of the polyhedrin gene.

Breakthrough in Microrobotics Reported

93P60104A Beijing ZHONGGUO DIANZI BAO [CHINA ELECTRONICS NEWS] in Chinese 30 Nov 92 p 3

[Article by Cai Tiewen [5591 6993 2429]: "Breakthrough Advance in Domestic Microrobotics Research"]

[Summary] An internationally unique microrobot drive apparatus, a two-coordinate microdrive and its control system, developed by Guangdong Institute of Technology Prof. Yang Yimin [2799 1355 3046], passed the technical appraisal held by the Natural Science Foundation of China a few days ago in Guangzhou. This apparatus, which uses piezoelectric components, has a two-axis common body, a circular-arc notch pivot point, and a computerized robust controller incorporating EMM [?electromagnetic measurement] techniques. Controllable accuracy is 0.03 μm, resolution is 0.01 μm, controllable run is 50 μm x 50 μm, drive force is 0.7 N, and bandwidth is over 400 Hz—values which take a leading position worldwide. The best resolution value heretofore reported worldwide was 0.5 μm, indicating that Prof. Yang's achievement is truly a breakthrough advance.

SAR Remote Sensing Applied Research Project Passes Acceptance Check

93P60105B Beijing KEJI RIBAO [SCIENCE AND TECHNOLOGY DAILY] in Chinese 14 Dec 92 p 2

[Article by Wu Yunsheng [2976 0061 3932]: "Synthetic Aperture Radar Remote Sensing Applied Research Breakthrough"]

[Summary] A key State S&T project involving applied research in synthetic aperture radar (SAR) remote sensing has achieved a breakthrough advance: at the recently concluded acceptance check, experts noted that the overall study has reached internationally advanced levels. Research in SAR remote sensing, used in such fields as geologic exploration, resources utilization, disaster detection, and military reconnaissance, was first included among State S&T Commission priority projects in 1989, and has been conducted over the past 3-plus years by the CAS Institute of Remote Sensing Applications and Institute of Electronics. The technology has been applied in the Tai Hu, Zhangjiakou, and Datong areas for geologic analysis; in the Jingjiang, Yongding He and Gu He rivers to analyze changes in the channels; and for flood detection/prevention in the Chu He area. In terms of radar system development, system parameter improvement, airborne radar remote sensing, radar imagery, and data processing/analysis, the experts have seen major achievements—propelling China into the world's front ranks in SAR development.

Flat Panel Color Large-Screen Display System Developed

93P60105A Beijing ZHONGGUO DIANZI BAO [CHINA ELECTRONICS NEWS] in Chinese 30 Nov 92 p 1

[Article by Lu Yuzhou [7120 3022 3166]: "Flat Panel Color Large-Screen Display System Developed"]

[Summary] A flat panel color large-screen display system with many attractive features such as high pixel density, good image definition, low operating voltage, lack of soft-X-ray emission, simple drive circuits, and a price much lower than that of comparable foreign-made products, was recently developed by the Huaguang Electronic Display Devices Plant in Shaoxing City, Zhejiang Province. This system, which incorporates the "color fluorescent picture tube" invented by Hangzhou University Prof. Ge Shichao [5514 0013 3390] and patented in the United States and China, has a pixel density 300-1,000 percent higher than that of a flood-beam tube, an anode voltage only one-tenth that of a flood-beam tube, a cost only one-tenth to one-twentieth that of a flood-beam tube, and a device depth only one-fourth that of a flood-beam tube, making it extremely competitive on the international market.

Further Reports on Pulsed Power Research

Design, Performance of 3.3 MeV LIA

93FE0122A Chengdu QIANG JIGUANG YU LIZI SHU [HIGH POWER LASER AND PARTICLE BEAMS] in Chinese Vol 4 No 3, Aug 92 pp 325-335

[Article by Cheng Nianan [4453 1819 1344], Zhang Shouyun [1728 1108 0061], et al., of Southwest Institute of Fluid Physics, Chengdu: "Design, Performance of 3.3 MeV LIA," supported by the National High-Technology Fund for Lasers; MS received 28 Jan 92, revised 4 May 92]

[Excerpts] Abstract: The physical appearance and measurement of characteristic beam parameters of a 3.3 MEV LIA (linear induction accelerator) are presented. All parameters measured have met or exceeded design specifications. It has been successfully used as the e-beam source for the SG-1 FEL (free electron laser). Presently, the plan is to serially connect more accelerating modules to it in order to raise the energy of the beam to 10 MeV so that it may be simultaneously used in FEL research and flash X-ray photography.

1. Introduction

This 3.3 MeV LIA is the e-beam source for the SG-1 FEL.[1] The design specifications of this 3.3 MeV LIA were confirmed by numerical computation of the SG-1 FEL using the WAGFEL code. The design work began in 1988 and system testing was completed in May 1991. The characteristic parameters include: electron energy E_e = 3.4 MeV (0.1 MeV higher than design value), beam current intensity I_b = 2 kA (0.5 kA higher than design), pulse width τ = 80 ns (20 ns higher than design), beam radius $R_b \leq 2$ cm (tunable, as designed), normalized emissivity ε_n = 0.6 πrad-cm (0.17 lower than design), beam brightness B_n = 10 kA/rad^2- cm^2 (5 kA/rad^2-cm^2 higher than design), and energy dispersion $\Delta\gamma/\gamma$ = 4% (1% below design). Between late May and the end of September 1991, this device was used to produce spontaneous amplification of radiation in the SG-1 FEL.

Figure 1 [photograph not reproduced] is a photograph of the 3.3 MeV LIA. The unit weighs approximately 3 tons and is mounted on a moving frame in the accelerator building of Southwest Institute of Fluid Physics. It is comprised of 12 accelerating modules in series. The first four modules act as an injector and the remaining eight form the accelerating part. Figure 2 shows the transverse layout of the 3.3 MeV LIA. The platform includes the accelerating cavity, Blumlein (B-line), main switch (level III switch) and pulsed power source. The accelerator control and monitoring systems are located in two rooms next to the main laboratory. The monitoring room is shielded against electromagnetic radiation. Ancillary systems for oil and deionized water treatment and gas (N_2 and SF_6) and vacuum handling are housed in a room outside the main building. Radiation protection has been taken into consideration in the design of the building. One can monitor the operation of the system in

the main building and the device on theplatform at the main control room via closed-circuit TV. A safety interlock device is in place to ensure personnel safety.

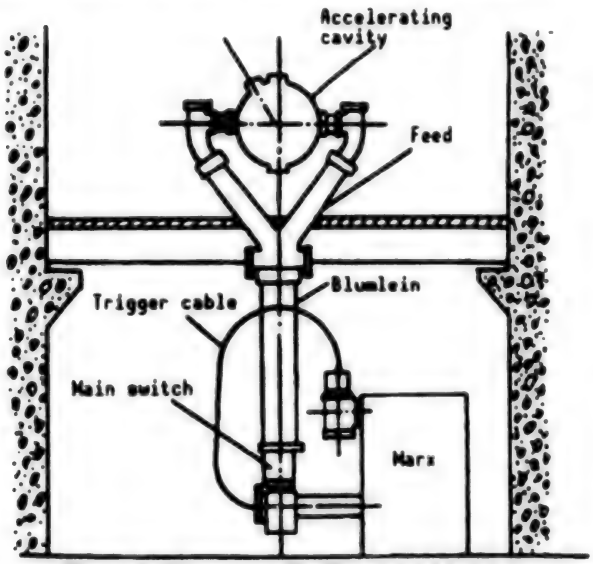

Figure 2. Transverse Profile of 3.3 MeV LIA

2. Physical Design and Study of Components

The 3.3 MeV LIA is comprised of accelerating modules, an injector, a pulsed power source and a beam transport system. Their design and construction was based on a single-module experimental unit and the development of a 1.5 MeV LIA. Nevertheless, because of the higher beam-current quality requirement, there were a number of technical hurdles and engineering problems, such as switch synchronization, design of a high-brightness injector, and effect of transport of intense beam on its quality. In the development process, Zhang Shouyun, et al., (1989) conducted investigations on these subjects to ensure that technical specifications were met and development schedules were kept.

2.1 Injector

The injector is a source which provides the accelerator with an e-beam of a certain quality. The quality of the injector directly affects the quality of the e-beam. In order to satisfy the brightness requirement of the SG-1 FEL, the beam brightness of the injector was investigated. The study was performed on a 1.5 MeV LIA (Figure 3). It was found that cathode material, anode and cathode structure, collimating ratio, and guiding magnetic field distribution affect beam brightness. Several cathode materials and cathode and anode structures were selected based on comparison and analysis for numerical computation. The results indicate that it is best to use a velvet cathode and adopt the structure shown in Figure 4. A brightness of 20 kA/(rad-cm)^2 could be obtained. In the meantime, an experimental study on the brightness of this kind of diode was conducted using the "pepper shaker" method with a magnetic collimator[2] and a brightness of 24 kA/(rad-cm)^2 was obtained. This is in good agreement with theoretical calculation.

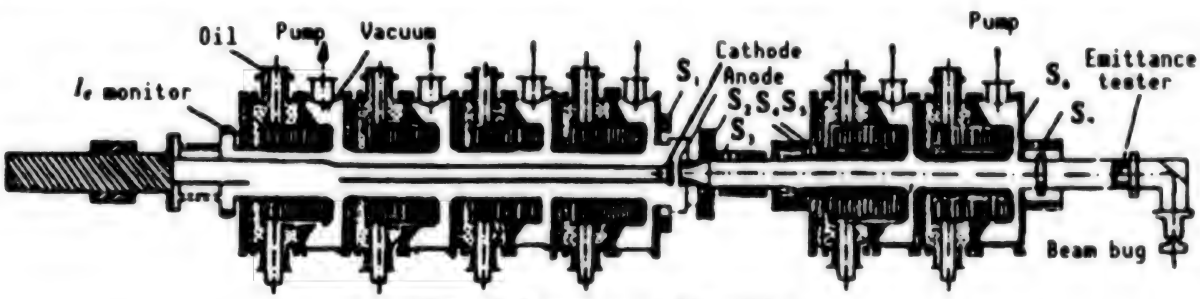

Figure 3. Schematic of 1.5 MeV LIA

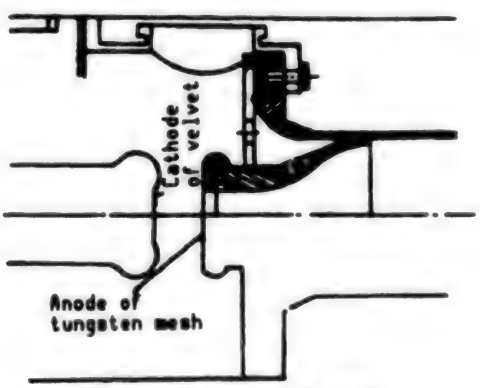

Figure 4. Schematic of Diode

The 3.3 MeV LIA has an additional six accelerating modules compared to the 1.5 MeV LIA. Based on the experimental result of the U.S. FXR accelerator, each module on average contributes to a 3 percent increase in emissivity. The six additional accelerating modules would lower beam brightness by 40 percent. Despite this, the beam brightness is still around 14 kA/(rad-cm)^2 to meet the need for research.

In addition, the effect of different collimating holes on brightness was investigated.[3] With a velvet cathode, a 2 cm collimating aperture produces a beam current of 1 kA and a brightness of 10^2kA/(rad-cm)^2. Numerical computation was done by replacing the diode with a pentode.

The result indicates that beam brightness can reach 10^2kA/(rad-cm)^2. This prepares us technically to meet and exceed the brightness specification of 5 kA/(rad-cm)^2.

2.2 Accelerating Modules

The 3.3 MeV LIA has a total of 12 accelerating modules. The front four serve as the injector and the rear eight act as the accelerating section. Figure 5 shows a cross section of the accelerating cavity. It includes a beam tube, focusing solenoid, MC nylon ring, stabilizing resistors and ferrite rings. Each module contains 14 ferrite rings, with major specifications as follows: 1) outer diameter 508 mm, inner diameter 254 mm, thickness 25 mm; 2) $B_s \geq 0.38$ T and $B_r > 0.28$ T at a magnetic field strength of 796 A/M; 3) maximum coercive force $H_c \leq 48$ A/M; 4) minimum resistivity $\rho \geq 3 \times 10^6$ Ω-cm; 5) voltage resistance: greater than 120 kV/25 mm (end) against 90-ns-wide voltage pulse (FWHM) in oil.

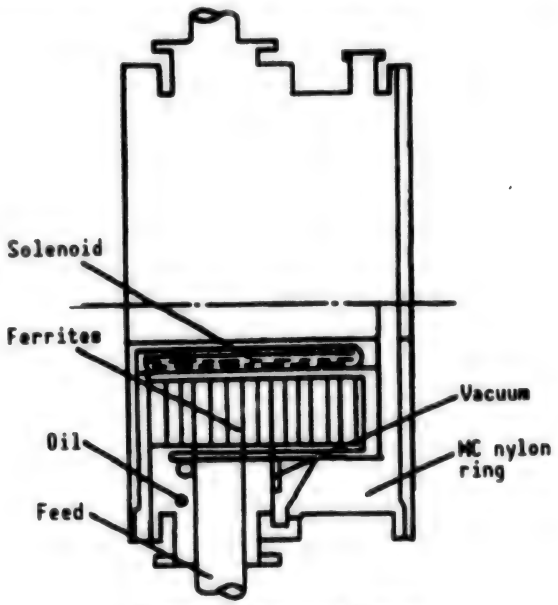

Figure 5. Schematic Cavity

The diameter of the vacuum e-beam transport tube is 146 mm and the acceleration gap is 45 mm. An MC-6 nylon ring is used to separate oil from vacuum. Copper sulfate solution resistors, stabilizing resistors, are installed perpendicularly above and below the feed to adjust the amplitude of the accelerating voltage and the complex current in the core of the magnet. A nonuniformly wound solenoid, capable of producing an axial magnetic field (B_z) of 0-0.2 T, is placed near the transport tube to confine the e-beam from diffusing while it is moving forward. Each accelerating cavity is equipped with a B-line (Blumlein). Every six B-lines are powered by a Marx generator. Each accelerating cavity is equipped with a voltage divider and a capacitor probe to monitor the accelerating voltage.

Based on past experience, some changes were made in the design of the accelerating cavity primarily to increase the axial distance of the solenoid in order to minimize any fluctuation caused by the separation of magnetic field in the accelerating gap. This is to ensure that the quality of the beam does not vary significantly in this region.

2.3 Pulsed Power Supply System

Figure 6 shows the pulsed power system for the 3.3 MeV LIA. Two Marx generators are used to resonantly charge 12 B-lines. A portion of the charging current passing through the B-line is used to reset the ferrites. When 90 percent of the charging voltage is reached, the trigger in each B-line is tripped and a pulse is delivered from the B-line via the feed to the accelerating cavity. Since its current is opposite in direction compared to the charging current, the ferrites are reversed to create a transition of magnetic flux which generates an accelerating voltage at the accelerating gap.

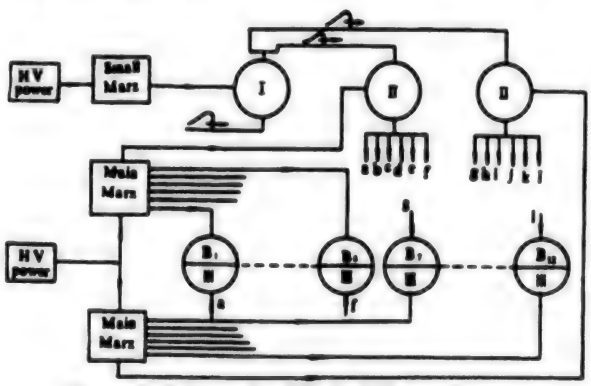

Figure 6. Schematic of Pulsed Power System

Key: I—first-stage switch; II—second-stage switch; III—third-stage switch; B—Blumlein

In order to synchronize the accelerating voltage and the e-beam in every accelerating cavity, a three-stage trigger system is used. A level-I switch simultaneously triggers two level-II switches and each level-II switch simultaneously triggers six main B-line switches. Synchronization is made possible by using different cable lengths between the level-II switch and main B-line switches and by properly adjusting the pressure in every switch. Identical level-III switches are used: they are three-electrode co-axial distortion spark-gap switches. Through numericalcomputation and experimental testing, it was found that using a mixture of N_2 and SF_6 as the insulating medium and at an operating voltage range of 120-300 kV, the tripping time of the switch could be controlled to within 1 ns by properly selecting the triggering pulse and adjusting the pressure.

The accelerating voltage is a function of the charging voltage of the Marx generator:

$$U_a = \left[\frac{4\eta C_M n U_0}{R_i (C_M + C_B)} - I_b\right] \frac{R_i R_L}{R_i + R_L} \quad (1)$$

where U_a is the accelerating voltage (kV), U_0 is the Marx charging voltage (kV), C_M is the output capacitance of the Marx, C_B is the total capacitance of the Blumlein, n is the order of the Marx, R_i is the internal resistance of the Blumlein, R_L is the stabilizing resistance, I_b is the beam current (kA), and η is the efficiency coefficient, which can be easily determined experimentally and is usually around 0.9.

2.4 Beam Transport System

During drifting and acceleration, it is unavoidable for an intense e-beam to suffer from some current loss and deterioration of quality due to factors such as space charge, magnetic field fluctuation, and transverse displacement of beam center. In serious cases, beam collapse might occur. The purpose of the beam transport system is to prevent and overcome various deleterious effects in order to minimize loss of brightness and beam quality to the extent possible. The transport system of the 3.3 MeV LIA employs a focused solenoid magnetic field, as shown in Figure 7. There are 17 solenoids (S_1-S_{17}); two pairs of coils of correction for beam station (SC), each pair consisting of two sets of X-Y transverse magnetic field coils; and three beam current and beam station probes (RBM). The magnetic field distribution for beam transport has taken the following factors into consideration. [Passage omitted]

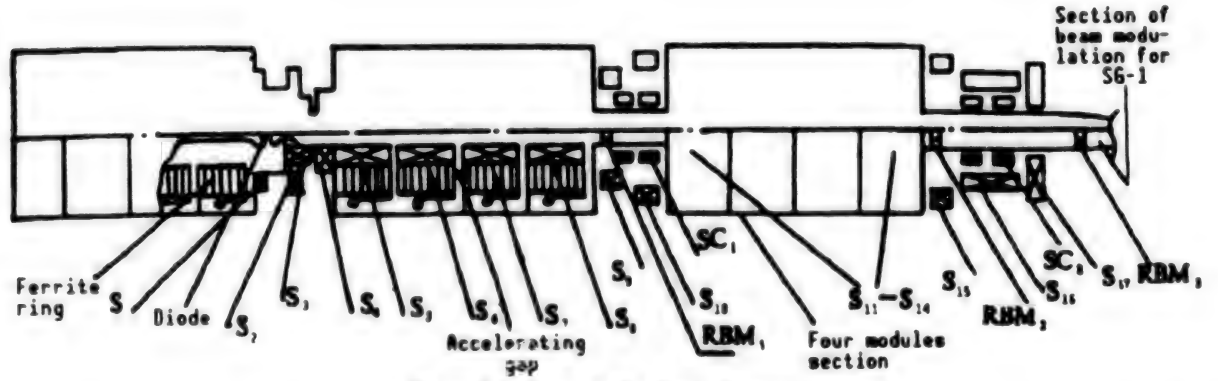

Figure 7. Schematic for Beam Transport

Key: RBM: probe of beam current and beam station; SC: coil of correction for beam station; S_1-S_{17}: solenoids of transport magnet for beam

With a beam energy of 3.33 MeV, beam current of 2.6 kA, and mean square root emissivity of 0.026 rad-cm, the magnetic field and beam-radius distribution have been computed using the SLAC-226 program (Figure 8). In the figure, solid lines are theoretical and dotted lines are experimental. They serve as a reference for tuning and testing. In the figure, z = 0 represents the cathode surface and circles are accelerating gap positions. In the experiment, the current in each coil is continuously tunable. The maximum magnetic field strength is as high as 0.2 T. Its stability is better than 0.1 percent and ripple is less than 0.1 percent. The requirements for theoretical estimation are completely met. As described earlier, certain modifications were made in the design of the module to reduce the magnetic field fluctuation in the accelerating gap from 50 percent to +/-12 percent. These changes created the conditions required to minimize the effect on brightness and to suppress instability during beam transport.

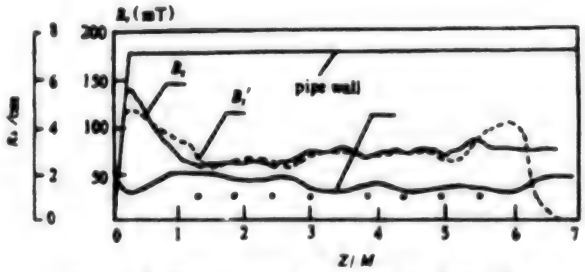

Figure 8. Distribution Curves of B_z With R_b

Solid line is theoretical value; dotted line is experimental value

3. Measurement of Accelerator Beam Characteristics

[Passage omitted] The appraisal team measured the beam characteristics of the 3.3 MeV LIA in October

1991. It was operated a total of 30 times. With the exception of two cases where synchronization was poor, the voltage and current profiles are essentially identical in the remaining 28 experiments. It operated steadily. A large amount of measurements demonstrate that the device has achieved the following specifications: beam current 2 kA, maximum energy 3.47 MeV, energy dispersion (base width) 3.7 percent, normalized emissivity 0.61 rad-cm, and normalized brightness 12.1 kA/rad^2-cm^2.

Presently, the accelerator has been moved 3 m transversely in order to assemble more modules into it for a 10 MeV unit. It is planned for use in flash X-ray photography as well. It is now in the tuning stage.

References

1. Hui Zhongxi [1920 6988 6932], "Design Study of the SG-1 FEL," QIANG JIGUANG YU LIZI SHU [HIGH POWER LASER AND PARTICLE BEAMS], Vol 2 No 3, 1990.

2. He Wenlong [0149 2429 7893], et al., "Measurement of Intense E-Beam Brightness Using Magnetic Collimator," QIANG JIGUANG YU LIZI SHU [HIGH POWER LASER AND PARTICLE BEAMS], Vol 2 No 2, 1990.

3. He Peiai [0149 1014 5337], et al., "Preliminary Investigation of Beam Quality Improvement With a Collimator," QIANG JIGUANG YU LIZI SHU [HIGH POWER LASER AND PARTICLE BEAMS], Vol 3 No 4, 1991.

4. Cheng Nianan, "Measurement of Emissivity of Strong Pulsed E-Beam," QIANG JIGUANG YU LIZI SHU [HIGH POWER LASER AND PARTICLE BEAMS], Vol 1 No 3, 1989.

Numerical Simulation of Vircator Oscillation for HPM Generation

93FE0122B Chengdu QIANG JIGUANG YU LIZI SHU [HIGH POWER LASER AND PARTICLE BEAMS] in Chinese Vol 4 No 3, Aug 92 pp 362-372

[Article by Wang Zhixiong [3769 4442 7160], Chen Yusheng [7115 7183 3932] and Fan Ruyu [5400 1172 3768] of Northwest Institute of Nuclear Technology: "Numerical Simulation of Virtual Cathode Oscillation for High-Power Microwave Generation"; MS received 30 Jul 91, revised 1 Dec 91]

[Excerpts] Abstract: The microwave generation process of an axially symmetric vircator (virtual cathode oscillator) is simulated. An ideal physical model is established based on the characteristics of the experimental setup. From the standpoint of fundamental laws of physics, a 2-1/2 dimension, fully electromagnetic, relativistic numerical simulation program involving two spatial dimensions and three momentum components is coded using the CIC method. A cylindrical electron beam is chosen in the simulation. Accurate results and crisp figures are obtained. The calculated results are also analyzed.

1. Introduction

The operating principle of a high-power microwave (HPM) device is to convert the kinetic energy of the e-beam to that of the radiation field. Its power is at least in the MW or GW range and the wavelength is in the microwave band. Compared to other HPM devices such as the relativistic magnetron, free electron laser, free electron maser, Cerenkov maser, gyrotron, plasma beam generator, backward-wave oscillator, and orotron, the vircator is simple in structure and convenient to tune and adjust. It is easy to arrange the microwave power output as well. The quality requirement of the e-beam is less stringent. Hence, it has more significance in practical use.

2. Analysis of Principle

There are two basic types of vircator. One is where the direction of microwave output is perpendicular to that of e-beam transport. With the exception of some experiments,[1,2] there has been almost no numerical simulation done on this kind of perpendicular-output mode because of its three-dimensional nature. The other is where the direction of microwave output is the same as that of e-beam transport. This kind of experimental setup (Figure 1) is axially symmetric and has been analyzed theoretically and simulated numerically in several papers.[3-10] A high-voltage negative pulse of the order of nanoseconds is applied to the cathode of a diode. The cathode is often made in the shape of a ring or cylinder. With the exception of foilless diodes, the anode is made of a metal foil or mesh. An axial guiding magnetic field may or may not be applied. Electrons from field-effect emission at the cathode are accelerated toward the anode. They penetrate the anode to enter the high-vacuum waveguide tube. When the current injected from the anode exceeds the limiting current of the waveguide tube, a virtual cathode is formed near the anode inside the waveguide tube. Its axial location is primarily determined by the kinetic energy and density of the injected electrons. In the virtual cathode region, a portion of the electrons continue to travel forward and are lost at the waveguide wall and electron absorber. Most electrons return to the anode and then reenter the diode region.

The virtual cathode is an area downstream from the anode where electrons are highly concentrated. It is the position where the electron kinetic energy is almost zero. In the virtual cathode area, the electron density is several times to several dozen times higher than the injection density. In conclusion, strong oscillation of high current density leads to the excitation of HPM. It has been demonstrated experimentally, as well as by way of theoretical simulation, that microwave generation can be further divided into the following two mechanisms. [Passage omitted]

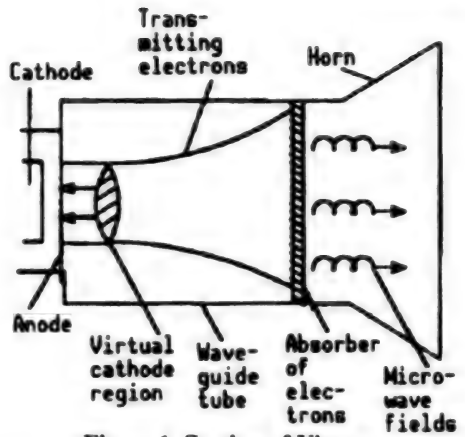

Figure 1. Section of Vircator

3. The Model

To facilitate numerical modeling, a semi-infinite, hollow metal tube waveguide with a radius r_w, as shown in Figure 2, is selected. An axially symmetric e-beam with an inner radius r_i and outer radius r_o is injected perpendicularly into the anode. Using the laboratory as the reference coordinate, the beam injection density is n_0, velocity is v_0 and there may or may not be a constant axial magnetic field. The electron absorber placed at L is used to absorb electrons transmitted through the virtual cathode. The transmission magnetic field has the same dielectric constant and magnetic susceptibility as those of vacuum. [Passage omitted]

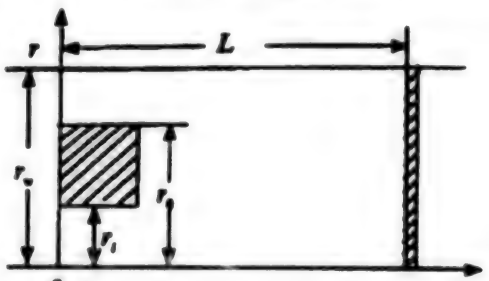

Figure 2. Simulation Arrangement and Coordinates

4. Results

It usually requires a high injection current density for a thin ring-shaped beam to form a virtual cathode. However, it is not so for a cylindrical beam. A cylindrical beam has a larger cross section. Even though the injection current density is low, a large injection current can be obtained to form a virtual cathode. The results of simulation of a cylindrical beam are as follows.

The simulation parameters are: $n_0 = 2.36 \times 10^{17}$ electrons/m^3, $\gamma = 2.57$, $r_i = 0$, $r_o = 8$ cm, $r_w = 14.4$ cm, $B_0 = 5T$ or $B_0 = 0$. Based on these parameters, it was calculated that $I_l = 7.2$ kA, $I_{in} = 210$ kA, $\omega_p = 2.74 \times 10^{10}$rad/s. In the following figures, unless noted otherwise, density, current density, current strength, time, and electric field are expressed in units of n_0, $-\gamma_0 J_0$, - 2.5 kA, 1.41 ps, and 4.26 MV/m, respectively. Here, $J_0 = en_0v_0$.

When a guiding magnetic field is present,($B_0 = 5T$, t = 9.87 ns), the virtual cathode is located at z = 1 cm (Figure 3). Compared to the case without the magnetic field ($B_0 = 0$, t = 9.87 ns), it is farther away (Figure 4). At the virtual cathode, electrons traveling in the -z and +z direction will concentrate to form a maximum density area. This density peak is primarily due to reflected electrons (Figures 3-4b). Although the peak density is a few to over a dozen times n_0, the negative J_z peak does not increase that much. Hence, the velocity of reflected electrons at the negative J_z peak is less, approximately 0.1-0.3 v_0.

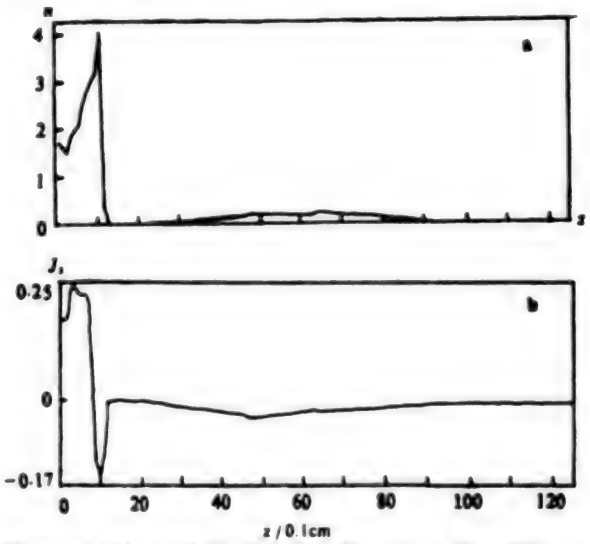

Figure 3. (a) Axial Distribution Density at $B_0 = 5T$, t = 9.87 ns, r = 3.8 cm (b) Axial Current Density Corresponding to (a). Abscissa unit: 0.1 cm

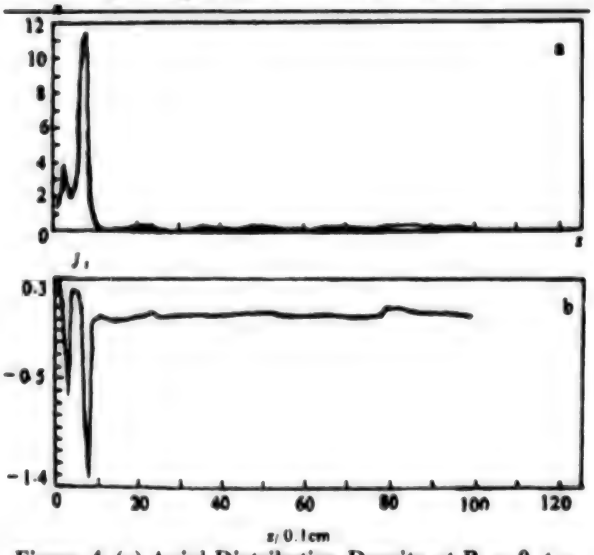

Figure 4. (a) Axial Distribution Density at $B_0 = 0$, t = 9.87 ns, r = 3.8 cm (b) Axial Current Density Corresponding to (a). Abscissa unit: 0.1 cm

The phase space snapshot of the e-beam and its cross section further illustrate the formation and spatial position of the virtual cathode (Figures 5-6). When B_0 = 5T, Ω/ω_g = 32, which is sufficient to limit the radial motion of the electron (Figure 5b). Because electrons rotate around the magnetic field, the beam quality is good. The beam also exhibits an apparent laminar flow behavior. The velocity of transmitted electrons is modulated by the microwave field. It vaguely reflects the microwave wavelength (Figure 5a). The beam quality is relatively poor without the guiding magnetic field (Figure 6b). Transmitted electrons hit the waveguide wall 30 cm downstream from the anode. Hence, only three-fifths of the total electrons exist in space compared to the case with B_0 present. Figure 6a fails to show any modulation of transmitted electron velocity.

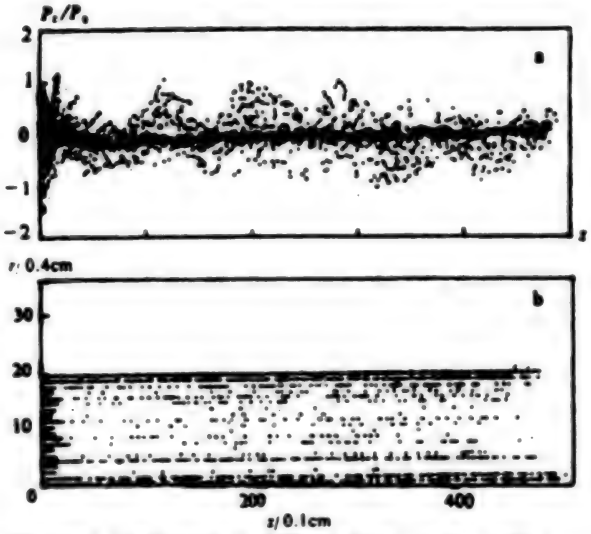

Figure 5. (a) Snapshot of Phase Space at B_0 = 5T, t = 7.05 ns, $P_0 = m_{e0}v_0$ (b) Section of Electrons at B_0 = 5T, t = 7.05 ns. Unit of ordinate r: 0.4 cm. Unit of abscissa z: 0.1 cm

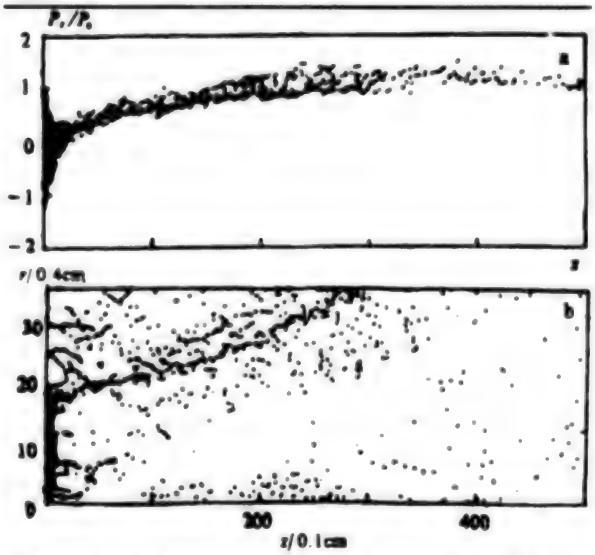

Figure 6. (a) Snapshot of Phase Space at B_0 = 0, t = 7.05 ns, $P_0 = m_e\gamma_0 v_0$ (b) Section of Electrons at B_0 = 0, t = 7.05 ns. Unit of ordinate r: 0.4 cm. Unit of abscissa z: 0.1 cm

Equation (2) [not reproduced], that estimates the transmitted current, is a static estimate with an infinite large guiding magnetic field and infinitely long waveguide. In reality, these conditions can only be partially met. Due to the formation of a virtual cathode, the dependence of transmitted current upon time is as shown in Figures 7 and 8. Regardless of the presence of a guiding magnetic field, it is easier for electrons at the outer fringe of the beam to penetrate the virtual cathode (Figures 5-6b). The time average for Figure 7 is 11.5 kA, higher than the estimated value of 7.2 kA derived from equation (2). Nevertheless, the time average for Figure 8 is only 1.4 kA. Obviously, such a difference is due to the lack of guidance for the transmitted electrons. The majority of transmitted electrons hits the waveguide wall 30 cm downstream from the anode (Figure 6b). Hence, equation (2) only reflects the mean transmitted current.

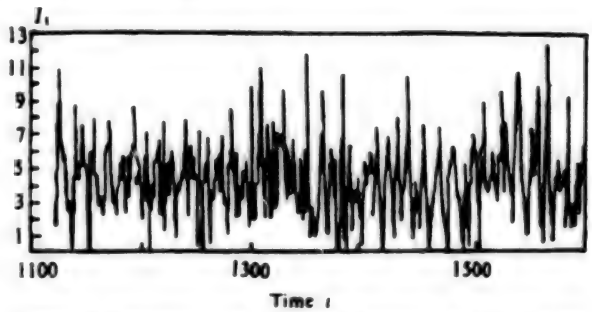

Figure 7. Dependence of Current Received at z = 45 cm on Time, B_0 = 5T

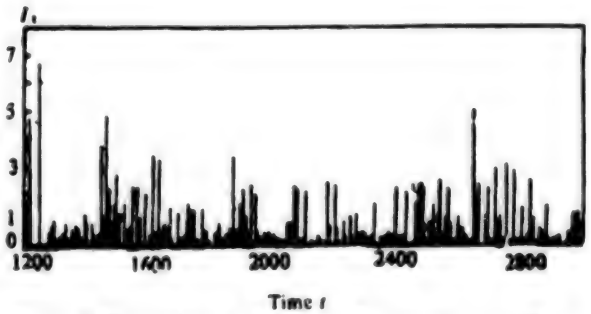

Figure 8. Dependence of Current Received at z = 45 cm on Time, B_0 = 0

The periodicity of virtual cathode oscillation is good with or without B_0. Two points are clearly illustrated by Figures 9a-d and 10a-c. One is that the position, charge and current density of the virtual cathode oscillate with time. The other is that an avalanche of incident electrons almost takes place at the virtual cathode. As an estimate, $\omega_v \approx (ne^2/\varepsilon_0 m_e \gamma)^{1/2}$ where n and γ are the electron density and relativistic factor in the virtual cathode, respectively. A review of Figures 9, 10a, 5 and 6a shows

that the minimum of n is n_0 and the maximum γ is γ_0. Where the electron density is the highest, $\gamma \approx 1$. Hence, the boundary for ω_v is

$$\omega_\perp \leq \omega_v \leq \omega_\perp n_{max}^{1/2} \gamma_0^{1/2} \qquad (7)$$

where n_{max} is the maximum spatial electron density, with units of n_0.

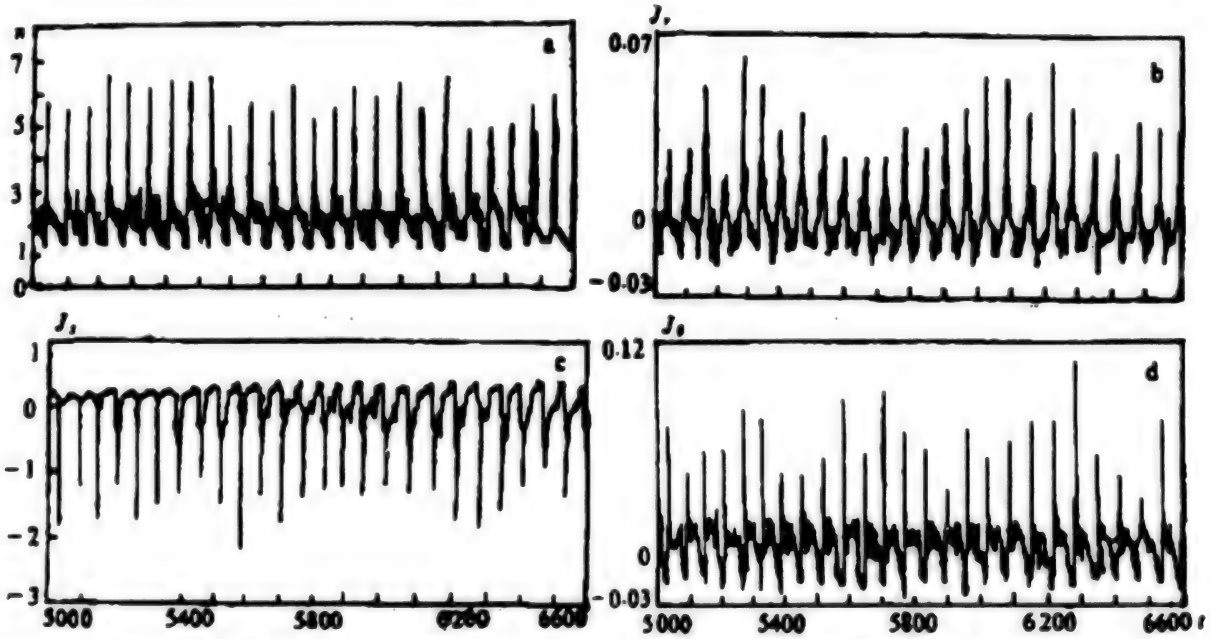

Figure 9. B_0 = 5T, Electron and Current Density Oscillations With Time at Fixed Space Points

(a) r = 5.8 cm, z = 0.25 cm; (b) r = 3.8 cm, z = 0.25 cm; (c) r = 3.8 cm, z = 0.35 cm; (d) r = 3.8 cm, z = 0.25 cm

Based on Figures 9a-d, the oscillation frequency of the virtual cathode is f_v = 11.3 GHz. This is higher than the 9.9 GHz value derived from Figures 10a-c without B_0. The reason is that the presence of the guiding magnetic field causes the number of spatial electrons to increase substantially. Consequently, more positive charges are induced on the anode surface. Hence, the electronic attractive force is stronger and the oscillation frequency is higher. From results obtained from simulation, the dependence of f_v upon B_0 is not significant. The frequency is lower at the beginning and it stabilizes after 1.4 ns. It is easy to verify that f_v obeys the $(I_{in}/I_l)^{1/4}\omega_p/2\pi$ law.

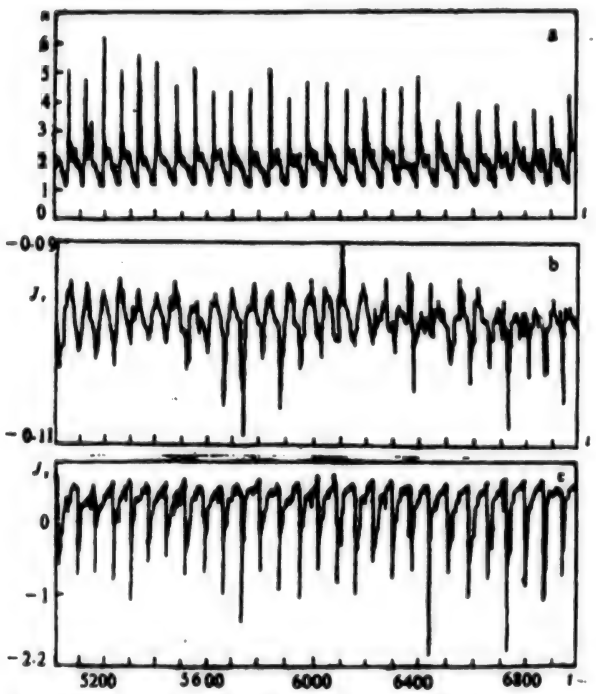

Figure 10. B_0 = 0, Electron and Current Density Oscillations With Time at Fixed Space Points

(a) r = 5.8 cm, z = 0.25 cm; (b) r = 3.8 cm, z = 0.25 cm; (c) r = 3.8 cm, z = 0.35 cm

The axial component of the current density, J_z, oscillates at a larger amplitude. It oscillates so strongly that it emits the TM wave. The frequency spectrum shown in Figure 11 indicates that the fundamental wave contributes the most. The first three harmonics also contribute a considerable portion. However, the dc component is very small. It is easy to determine that the fundamental frequency is at 9.9 GHz.

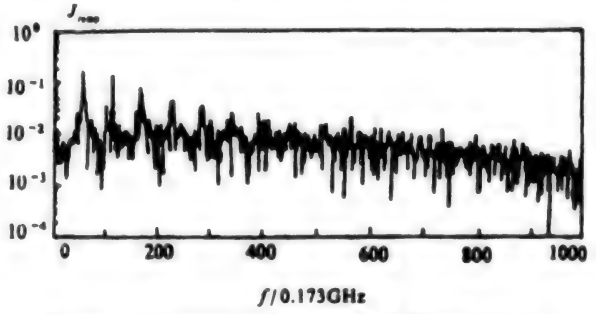

Figure 11. Frequency Spectrum of Figure 10(c), Abscissa Unit: 0.173 GHz

Virtual cathode oscillation generates microwave radiation (Figures 12- 14). The frequency spectrum of E_θ has a sharp peak at 11.3 GHz. Its amplitude is much smaller than E_z. The primary part is the TM wave. When B_0 =

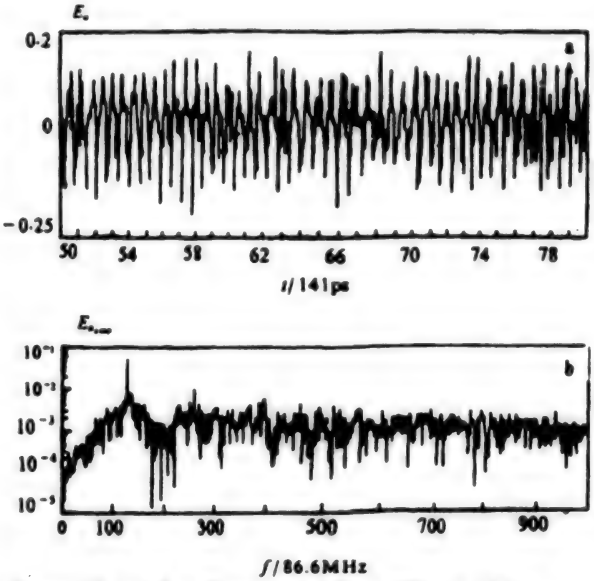

Figure 12. (a) E_0-t Diagram at B_0 = 5T, r = 13 cm, z = 5 cm, Time Unit: 1.41 x 10^{-10}s (b) Frequency Spectrum Corresponding to (a). Frequency unit: 8.66 x 10^7Hz

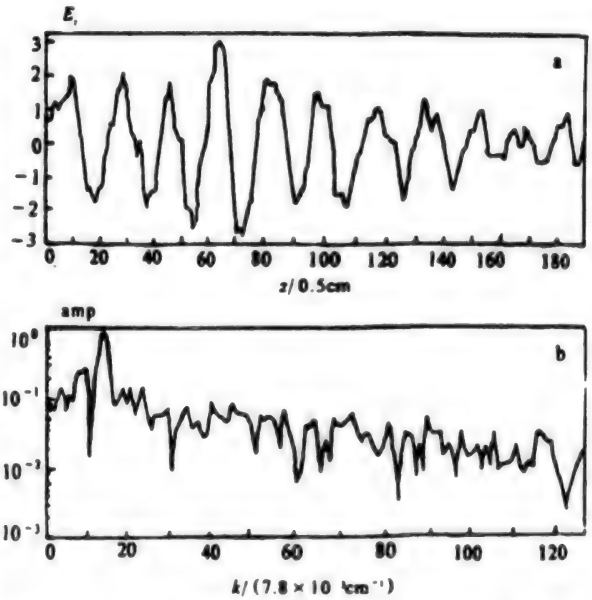

Figure 13. E_z - z Diagram at t = 9.87 ns, r = 13 cm. (b) Wave Number Spectrum Corresponding to (a).

B_0 = 5T, z and k in units of 0.5 cm and 7.8 x 10^{-3}cm^{-1}

5T, the TM wave has an apparent major wavelength (Figure 13). There is a peak at wave number k = 14.3, corresponding to a wavelength of λ = 9 cm. In the absence of B_0, the distribution of TM wavelength is more scattered (Figure 14); the major wavelength seems to be

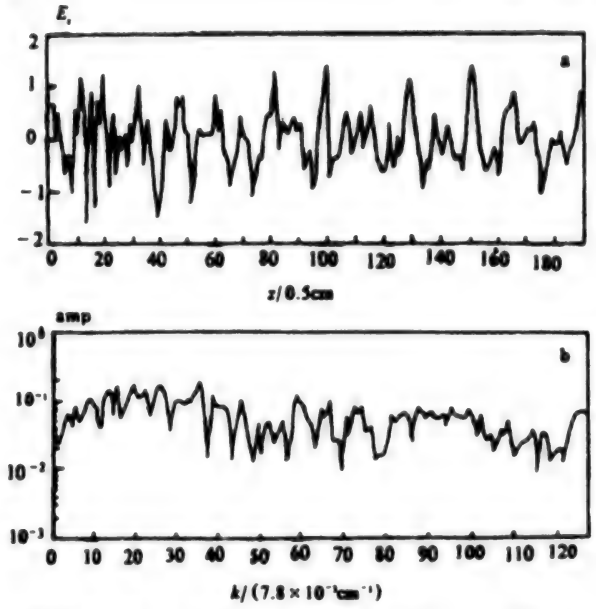

Figure 14. E_z - z Diagram at t = 9.87 ns, r = 13 cm. (b) Wave Number Spectrum Corresponding to (a).

B_0 = 0, z and k in units of 0.5 cm and 7.8 x $10^{-3}cm^{-1}$

3.7 cm. As far as the TM_{0n} wave, which is a simple harmonic oscillation at an angular frequency ω, is concerned, the dispersion of the waveguide is

$$\gamma_{0n}^2 = \frac{\omega^2}{c^2} - \left(\frac{2\pi}{\lambda_{0n}}\right)^2 \quad (8)$$

where $\gamma_{On} = \eta_{On}/r_w$. η_{On} and λ_{On} are the nth root of zero-order Bessel function and wavelength of the TM_{On} wave, respectively. Hence, it can be concluded that a guiding magnetic field can produce a relatively pure TM wave in terms of frequency, wavelength and mode by means of cathode oscillation. Otherwise, even single-frequency oscillation can produce multiple modes in the waveguide due to the fact that the wavelength is scattered. The radial distribution of E_z is similar to the zero-order Bessel function $I_0(\gamma_{On}r)$ (Figure 15).

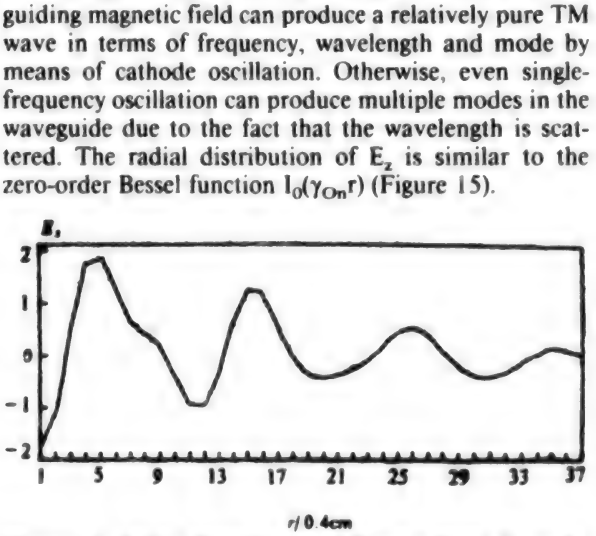

Figure 15. Radial Distribution of Electric Field E_z at B_0 = 5T, t = 12.69 ns, z = 195 cm. Abscissa unit: 0.4 cm

The field inside the waveguide is a superposition of the radiation field and electron field. The electron field can be neglected only at places far away from the source. The energy flux is $S = ExB/\mu_0$ and the total radiation power is P_t = integral of S x e_3dA, where μ_0 is the magnetic susceptibility in vacuum, e_3 is a unit vector in the z direction and the integral covers the entire cross section of the waveguide. P_t can be expressed as the sum of the total power of TM and TE waves, i.e., P_{tm} and P_{te}, or $P_t = P_{tm} + P_{te}$. P_{tm} = integral of E_rB_0/μ_0dA and P_{te} = integral of $-E_\theta B_r/\mu_0$dA. The simulation shows that the power of TE waves is far less than that of TM waves when B_0 = 5T. The mean values are 3.5 GW and 1.2 GW, respectively. When B_0 = 0, the mean TM wave power is 0.6 GW. Therefore, it is obvious that the presence of a guiding field is desirable for microwave radiation.

The above results have been obtained under ideal conditions. In a real vircator, due to the presence of electromagnetic waves transmitted through the anode and returned electrons, both excitation mechanisms exist simultaneously. ω_v should be lower than the simulated result. The e-beam injected from the anode cannot possibly be a totally cold beam. It must have a rising edge and a falling edge. The beam current would be neutralized by plasma formation on the cathode and the subsequent plasma acceleration. It is also impossible to have a zero-loss waveguide wall. These factors more or less would affect the microwave.

4. Conclusions

When the radius of a cylindrical beam

$$2r_0 > \sqrt{\frac{\gamma_0(\gamma_0-1)}{\gamma_0+1}}\ \frac{c}{\omega_p},$$

equation (1) provides an excellent theoretical estimate. The return of electrons produces peaks in the density distribution. The beam fringe can easily penetrate the virtual cathode and contributes more to the transmitting current. The transmitting current is a function of time and its average value is higher than the static value provided by equation (2). The presence of a guiding magnetic field can significantly improve the quality of the beam. ω_v obeys the$(I_{in}/I_l)^{1/4}\omega_p$ law and its lower limit is still $\omega_{perp.}$. The dependence of ω_v upon B_0 is not significant; ω_v increases slightly as B_0 rises. The microwave generated by vircator oscillation is primarily concentrated on the TM mode. A guiding field can benefit microwave radiation.

Acknowledgement

The authors wish to thank Chen Yanqiao [7115 4291 2890], et al., for their valuable opinions.

References

1. Sze, H., et al., "Dynamics of a Virtual Cathode Oscillator Driven by Pinched Diode," PHYS. FLUIDS, Vol 29 No 11, 1986, p 3873.

2. Mahaffey, R.A., et al., "High-Power Microwaves From a Nonisochronic Reflecting Electron System," PHYS. REV. LETT., Vol 39, 1977, p 843.

3. Kwan, T.J. T., "High-Efficiency, Magnetized, Virtual-Cathode Microwave Generator," Ibid., Vol 57 No 15, 1986, p 1895.

4. Kwan, T.J. T. and Thode, L.E., "Formation of Virtual Cathodes and Microwave Generation in Relativistic Electron Beams," PHYS. FLUIDS, Vol 27 No 7, 1984, p 1570.

5. Kwan, T.J. T., "High-Power Coherent Microwave Generation From Oscillating Virtual Cathodes," Ibid., Vol 27 No 1, 1984, p 228.

6. Abraham Kadish, et al., "Analysis and Simulation of Virtual Cathode Oscillations," Ibid., Vol 29 No 12, 1986, p 4192.

7. Thode, L.E., et al., "Vacuum Propagation of Solid REBS," Ibid., Vol 22 No 4, 1979, p 747.

8. Wee-yong woo, "Two-Dimensional Features of Virtual Cathode and Microwave Emission," Ibid., Vol 30 No 1, 1987, p 239.

9. Davis, H.A., et al., "High-Power Microwave Generation From a Virtual Cathode Device," PHYS. REV. LETT., Vol 55 No 21, 1985, p 2293.

10. Burkhart, S.C., et al., "A Virtual-Cathode Reflex Triode for High- Power Microwave Generation," J. APPL. PHYS., Vol 58 No 1, 1985, p 28.

11. Poukey, J.W. and Rostoker, N., "One-Dimensional Model of Relativistic Electron Beam Propagation," PLASMA PHYSICS, Vol 13, 1971, p 879.

Laser in Neon-Like Germanium Plasmas

40100051A Chengdu QIANG JIGUANG YU LIZI SHU [HIGH POWER LASER AND PARTICLE BEAMS] in Chinese Vol 4 No 4, Nov 92 pp 521-530

[English abstract of article by Zhang Guoping, Sheng Jiatian, et al. of the Institute of Applied Physics and Computational Mathematics, P.O. Box 8009, Beijing, 100088, and Yu Min of China Academy of Engineering Physics, Chengdu, 610003; MS received 7 Apr 92, revised 16 Jun 92]

[Text] In order to prevent the laser beam from being refracted out of lasing medium, we proposed and carried out a novel design named double-target opposing coupling (early 1990). We developed opposing coupling idea and proposed following coupling idea for four-target series coupling experiments in early 1991. The total length for four targets is up to 5.6 cm. We have developed a series of codes, which can simulate the laser-produced plasma condition, population inversion, gain of laser lines, and propagation and amplification of laser lines in lasing medium. Before these four-target series coupling experiments, we adjusted some parameters in JB19 and ALPHA codes in order to match the results of last double-target opposing coupling experiments. The results of simulation for laser line of 23.2 nm agree with those of the last round experiment. Then we simulate this round of experiment and get the parameters of the distance and angle between the targets in order to get best coupling. The results of the experiments show that the simulation is good. The gain length product (GL) of small signal is up to about 18 for both lines at 23.2 and 23.6 nm, and the effective GL is 16.4 and 15.7 for these two lines, respectively. These two lines are obviously tending to saturation. The divergence of laser beams reduces to 3-4 mrad.

Sensitive GaAs Detectors and Applications

40100051B Chengdu QIANG JIGUANG YU LIZI SHU [HIGH POWER LASER AND PARTICLE BEAMS] in Chinese Vol 4 No 4, Nov 92 pp 575-580

[English abstract of article by Yang Xiangdong, Liu Shenye, Li Chaoguang, Zheng Zhijian, and Tang Daoyuan of the Southwest Institute of Nuclear Physics and Chemistry; MS received 25 Feb 92, revised 1 Jun 92]

[Text] In ICF experiments, we have applied newly developed small GaAs-photoconductor detectors made with neutron-treated GaAs crystal material. Hard X-ray signals and hard X-ray angular distribution have been obtained with the detectors. The sensitivity to the X-rays is about 10^{-18} C/keV and the response about 100 ps. The detectors have the ability to resist electromagnetic radiation inferfering in the target chamber.

Investigations of Main Microwave Mode Excited by Virtual Cathode Formed by Hollow Electron Beams

40100051C Chengdu QIANG JIGUANG YU LIZI SHU [HIGH POWER LASER AND PARTICLE BEAMS] in Chinese Vol 4 No 4, Nov 92 pp 600-604

[English abstract of article by He Yiping, Chen Deming, Lin Gensheng, Liu Yonggui, and Li Chuanlu of the Department of Applied Physics, National University of Defense Technology, Changsha, Hunan, 410073; MS received 18 Sep 91, revised 15 Jun 92]

[Text] The process of virtual cathode oscillation exciting microwaves is considered as that of an oscillating current element exciting microwaves. With the approximation of thin charge sheet, the criterion of the main mode of the excited microwave is obtained. The relation between the beam dimension and the output power is discussed. Our criterion is in agreement with that of experiments and particle simulations.

Studies of Miniature Optically Pumped Far-Infrared Laser

40100047A Beijing DIANZI XUEBAO [ACTA ELECTRONICA SINICA] in Chinese
Vol 20 No 11, Nov 92 pp 39-44

[English abstract of article by Luo Xizhang and Lin Yikun, Department of Electronics, Zhongshan University, Guangzhou 510275,MS received Jul 91, revised Oct 91]

[Text] Based on the density matrix equations of three-level NH_3 molecular system, power density of FIR laser from mini- OPFIRL was calculated numerically by iteration method. Five OPFIRLs with sample tube 10 cm, 5 cm, 4.3 cm, 3 cm and 1.5 cm in length, respectively, lase successfully. Longitudinal cavity effect and transverse feedback effect are proved to be active in mini-OPFIRL, and have important effects on the optimum operating gas pressure and spectral characteristic of mini-OPFIRL.

Experimental Study of Actively Mode-Locking Semiconductor Laser With External Grating Cavity

40100047B Beijing DIANZI XUEBAO [ACTA ELECTRONICA SINICA] in Chinese
Vol 20 No 11, Nov 92 pp 45-50

[English abstract of article by Xu Changcun, Guan Yichun, Guo Yiji, and Zhan Yushu, Xidian University, Xi'an 710071; MS received Jun 91, revised Jan 92]

[Text] The properties, such as output pulse width and spectrum of actively mode-locking semiconductor laser with an external grating cavity are studied in detail. The optimization process of the parameters of the device influencing the pulse width is given. With sinusoidal microwave modulation, a fully mode-locked pulse train is obtained with the FWHM as short as 8.2 ps, repetition frequency 961.06 MHz, peak power greater than 150 mW and tuning range greater than 10 nm.

MBE Ultrathin-Layer Microstructure Materials Research Facility Gives Demonstration

93P60112A Beijing ZHONGGUO KEXUE BAO [CHINESE SCIENCE NEWS] in Chinese 4 Dec 92 p 2

[Article by Liu Li [0491 0500]: "Semiconductor Ultrathin-Layer Microstructure Materials Research Base Passes Expert Demonstration Test"]

[Summary] Beijing, ZHONGGUO KEXUE BAO wire report—On 15 October, the MBE [molecular beam epitaxy] ultrathin-layer microstructure materials research facility jointly constructed by the "863 Plan" New Materials Area Expert Commission and the CAS Semiconductor Materials Science Laboratory passed an expert demonstration test. This new facility, which will concentrate on optoelectronic and microelectronic devices, has imported advanced MBE equipment from overseas in an effort to conduct state-of-the-art research and development, and to reduce product lead times.

Details Released on DYL Multielement Logic Circuits With Subnanosecond Gate Delay

93P60098A Dalian DALIAN LIGONG DAXUE XUEBAO [JOURNAL OF DALIAN UNIVERSITY OF TECHNOLOGY] in Chinese Vol 32 No 6, Nov 92 pp 644-652

[Article by Zou Helin [6760 6378 7792], Wei Xiwen [7614 1585 2429], and Ma Pingxi [7456 1627 6007], Department of Physics: "Development of Subnanosecond-Speed High Uniformity Multielement Logic Circuits"; MS received 16 Oct 91, revised 1 Sep 92]

[Abstract] Simultaneous achievement of high speed and high uniformity in the DYL (duoyuan luoji, "multielement logic") series of domestically invented bipolar logic ICs[1-4] is discussed by theoretical analysis and experiment. The basic function of the DYL chips is as a linear AND/OR gate, which has both digital input (logic) and linear analog doubling functions. These chips have important applications in multivalue logic circuits, high-speed multipliers, and analog signal delay lines. Sample circuits—the DYL-3, a 28-pin, 1.4 mm x 1.4 mm eight-bit controllable two-input AND gate with minimum photoetching line width of 4 μm, minimum registration spacing of 2 μm, and emitter junction area of 8 μm x 8 μm, and the DYL-4, a 28- pin, 1.2 mm x 1.0 mm eight-bit D/A AND/OR gate, with minimum photoetching line width of 4 μm, minimum registration spacing of 3 μm, and emitter junction area of 14 μm x 10 μm, the two chips forming the linear AND/OR gate—are trial fabricated by a double-base, double-emitter shallow-junction diffusion silicon planar technique. Testing of 250 samples shows that the DYL-3 has an average single-gate delay of 0.22 ns and power consumption-delay product of 0.55 pJ, while the DYL-4 has an average single-gate delay of 0.24 ns and power consumption-delay product of 0.60 pJ. On condition of identical input (0-4 V), output uniformity of each gate is less than or equal to 4 mV. These results indicate that the DYL circuits form an excellent high-speed, high-uniformity linear logic switching gate.

The DYL-3 and DYL-4 equivalent circuits are shown below in Figures 6 and 7, respectively, while the chip layouts are shown in Figures 8 and 9. Figures 1-5 and 10-12 [not reproduced] show various equivalent circuits, parameter relationship, the gate-delay testing circuit, and

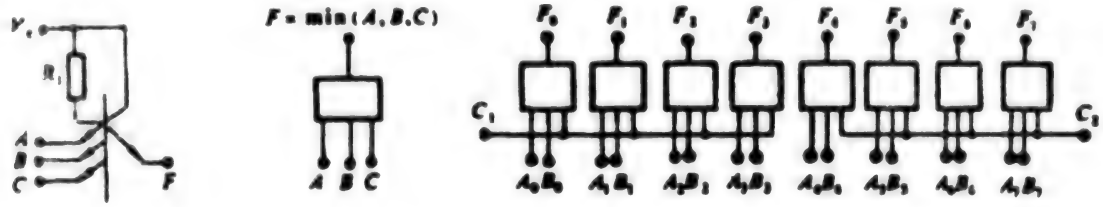

(a) Cell circuit (b) Circuit symbols (c) Overall circuit

Figure 6. 8-Bit Controllable 2-Input AND Gate (DYL-3)

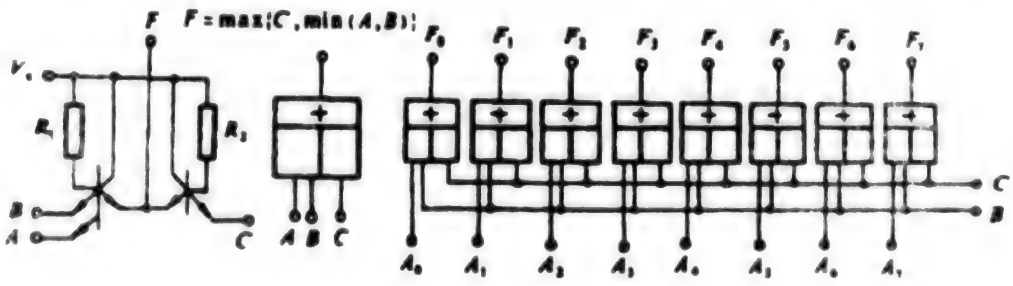

(a) Cell circuit (b) Circuit symbols (c) Overall circuit

Figure 7. 8-Bit D/A AND/OR Gate (DYL-4)

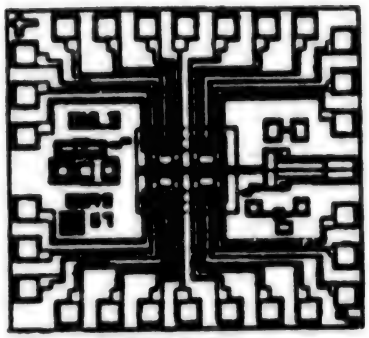

Figure 8. DYL-3 Chip Layout

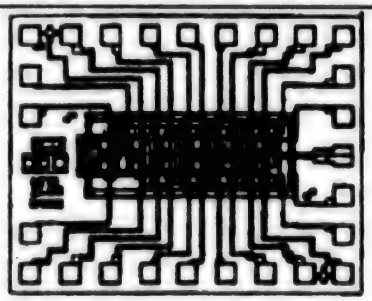

Figure 9. DYL-4 Chip Layout

oscilloscope plots, while three tables [not reproduced] list details of the gate delay and uniformity for both chips.

References:

1. Wang Shoujue, Sun Xiangyi, and Wang Runmei, "A New High-Speed Integrated Logic Circuit," DIANZI XUEBAO [ACTA ELECTRONICA SINICA], Vol 6 No 2, 1978, pp 43-51.

2. Wang Shoujue, "New Techniques for Providing Continuous Logic in Electronic Circuits and Systems," Ibid., Vol 14 No 5, 1986, pp 1-11.

3. Shi Yan and Wang Shoujue, "D/A Converter With DYL Null-Point- Determination Analog Switch," Ibid., Vol 16 No 5, 1988, pp 48-54.

4. Wang Shoujue, Shi Yan, and Zhu Ronghua, "Multielement-Logic 12-Bit x 12-Bit Very-High-Speed Multiplier," BANDAOTI XUEBAO [CHINESE JOURNAL OF SEMICONDUCTORS], Vol 8 No 5, 1987, pp 466-473.

5. Zou Helin, "Study of High-Speed Multielement Logic Circuits," Academic Treatise, Dalian: Dalian University of Technology, 1989.

6. Narud, J.A. and Meyer, C.S., "Characterization of Integrated Logic Circuits," PROC. IEEE, Vol 52 No 12, 1964, pp 1551-1564.

New Method for Revealing Defects in GaAs/AlGaAs—Ultrasonic-Aided AB Etching

40100050A Beijing BANDAOTI XUEBAO [CHINESE JOURNAL OF SEMICONDUCTORS] in Chinese Vol 13 No 12, Dec 92 pp 763-766

[English abstract of article by Chen Nuofu of Hebei Institute of Technology, Tianjin, 300130; MS received 14 Aug 91, revised 31 Oct 91]

[Text] A new method for revealing various defects in GaAs/AlGaAs by means of Ultrasonic-Aided AB Etching (USAB) is presented. The emergent dislocations, dislocation lines, stacking faults, microdepositions, and growth-induced striations can all be revealed with this method under natural light and room temperature

Efficient Infrared-Upconversion Luminescence in Porous Silicon: Quantum-Confinement-Induced Effect

40100050B Beijing BANDAOTI XUEBAO [CHINESE JOURNAL OF SEMICONDUCTORS] in Chinese Vol 13 No 12, Dec 92 pp 773-776

[English abstract of article by Wang Jian, Jiang Hongbing, Wang Wencheng, and Zheng Jiabiao of the Joint Laboratory for Materials Modification by Laser, Ion and Electron Beams (Fudan Branch), Fudan University, Shanghai, 200433; Zhang Fulong, Hao Pinghai, Hou Xiaoyuan, and Wang Xun of the Surface Physics Laboratory (State Key Laboratory), Fudan University, Shanghai, 200433; MS received 6 May 92, revised 3 Jul 92]

[Text] We demonstrate for the first time that the porous silicon layer (PSL) which has a bright light-emission band in the range 500-700 nm exhibits a strong visible-range luminescence under the illumination of infrared ultrashort-pulse laser. The intensity dependence of integrated luminescence on pump power shows that this is a third-order nonlinear optical effect. By comparing with UV-light-excited spectra of PSL and samples with low porosity which have inefficient luminescence, a possible explanation that the large nonlinear optical response is due to the quantum-confinement effect has been proposed.

300kW-Class Superconducting Single-Stage Electric Machine Unveiled

93P60115A Beijing RENMIN RIBAO [PEOPLE'S DAILY OVERSEAS EDITION] in Chinese 7 Jan 93 p 1

[Unattributed article reprinted from CHANG JIANG RIBAO: "Nation's First Superconducting Single-Stage Electric Machine Unveiled"]

[Summary] Wuhan, 6 Jan (XINHUA)—The nation's first superconducting single-stage electric machine, with a 300 kW power rating, has been unveiled. According to published foreign S&T information as of the end of 1991, only Britain and the United States had developed 300kW-class single-stage electric machines. This new machine, developed over a 9-year period by 30 engineers in the Superconductivity Laboratory at the China State Shipbuilding Corporation's Institute 712, held a power of 300 kW for 36 minutes under loaded operating conditions, and has a maximum experimentally measured power of 331.3 kW.

Superconducting Films of $Tl_mBa_2Ca_nCu_{n+1}O_y$ Prepared by Dip-Coating Method

40100045A Beijing DIWEN WULI XUEBAO [CHINESE JOURNAL OF LOW TEMPERATURE PHYSICS] in Chinese Vol 14 No 6, Nov 92 pp 429-432

[English abstract of article by Wang Jian and Cheng Jijian, Department of Ceramics, The East China Institute of Chemical Engineering, Shanghai 200237; MS received 8 Feb 92]

[Text] Oriented superconducting films of $Tl_mBa_2Ca_nCu_{n+1}O_y$ (m = 1,2; n = 1,2) were prepared by dip-coating method using acetate as starting materials. The relationship between the crystalline phase and the composition of the films was studied. When Tl/Ba ratio in the films was greater than 0.7, double Tl-layer compounds (m = 2) were obtained. Otherwise, single Tl-layer compounds were obtained. The thickness of the films prepared in this paper was about 2 μm. The maximum T_{co} (critical temperature) and J_c (critical current density, 77K, 0T) values of double Tl-layer compounds were 110K and 1.8 x 10^4A/cm^2, respectively.

Study of YBCO Superconducting Ceramics With Dopant SnO_2

40100045B Beijing DIWEN WULI XUEBAO [CHINESE JOURNAL OF LOW TEMPERATURE PHYSICS] in Chinese Vol 14 No 6, Nov 92 p 450-454

[English abstract of article by Chen Ang and Zhi Yu, Department of Physics, Zhejiang University, Hangzhou 310027; and Li Biaorong and Zhang Xuli, Department of Solid State Electronics, Huazhong University of Science and Technology, Wuhan 430047; MS received 21 Nov 91]

[Text] The doping effect of the additive SnO_2 on the manufacturing procedure, sintering mechanism, microstructure and superconductivity of $YBa_2Cu_3O_y$ ceramics was studied. For optimum contents of dopant SnO_2, the sintering quality was improved, fine and dense microstructure of ceramics were obtained, and the critical current density of the superconducting ceramics was obviously increased. A brief discussion about the experimental results is given.

High-T_c Thin Film Edge Weak Link Junctions

40100045C Beijing DIWEN WULI XUEBAO [CHINESE JOURNAL OF LOW TEMPERATURE PHYSICS] in Chinese Vol 14 No 6, Nov 92 pp 472-474

[English abstract of article by Wang Huabing, Zhang Hui, et al., Department of Information Physics, Nanjing University, Nanjing 210008; MS received 22 Nov 91]

[Text] Fabrication of characterization of high-T_c YBCO thin-film edge junctions is reported. Both layers of the YBCO thin films used in the edge junctions are fabricated through DC magnetron sputtering with a zero-resistance temperature of more than 80K. The current-voltage characteristics of the edge junctions show a zero-voltage supercurrent at 78K and some Shapiro steps at 70K under 36 GHz microwave irradiations.

MMEI Vice Minister Speaks at HDTV Development Symposium

93P60108B Beijing ZHONGGUO DIANZI BAO [CHINA ELECTRONICS NEWS] in Chinese 11 Dec 92 p 1

[Article by Liu Dong [0491 2639] and Jin Jianzhong [6855 1696 0022]: "Beijing Holds High-Definition Television Development Symposium; Zeng Peiyan Proposes Development Concepts, Targets"]

[Summary] The Beijing 2000 Olympic Games High-Definition Television (HDTV) Development [International] Symposium was held in Beijing on 5-7 December by the Ministry of Machine-Building and Electronics Industry (MMEI), the Ministry of Radio, Film and Television (MRFT), the State Physical Education Commission (SPEC), and the Beijing Olympic Games Preparation Committee. It has already been decided by relevant Chinese organizations and the International Olympic Committee that some HDTV programs will be broadcast to the world from the Beijing 2000 Olympics, and MMEI Vice Minister Zeng Peiyan addressed the group on strategic thinking and development targets to be kept in mind by the various Chinese and foreign planners in order to provide this HDTV service. For China itself, Vice Minister Zeng proposed the following HDTV development targets for the year 2000: determination of an HDTV laboratory standard and transmission system, initial construction of an HDTV receiver manufacturing base, construction of an HDTV trial-broadcast system for broadcasting programs to the world, and gradual permeation of HDTV technology applications into the economy. MMEI, MRFT, and SPEC announced that they have submitted a report entitled "Development of China's HDTV System Equipment" to the State Council. In addition to the aforementioned groups, representatives from [the Netherlands'] Philips, the Taiwan Industrial Technology Research Institute, Hong Kong's Keyuan [4430 5373] and Kehui [4430 0565] companies, Qinghua University, Tianjin University, the Beijing Institute of Posts and Telecommunications, Chengdu University of Electronic Science and Technology, Xidian University, and the Beijing Mudan [3665 0030] Electronics Group gave product demonstrations or delivered special reports. Representatives from the State Planning Commission, State Science and Technology Commission, and Ministry of Finance also attended the symposium.

Sino-Japanese Optical Fiber Project Agreement Reached

93P60108A Beijing ZHONGGUO DIANZI BAO [CHINA ELECTORNICS NEWS] in Chinese 9 Dec 92 p 1

[Article by Gu Bingxin [7357 3521 9515] and Liu Hua [0491 5478]: "Sino-Japanese Cooperative Optical Fiber Project Signed"]

[Text] On 19 November, agreement was formally reached on a Sino-Japanese optical fiber cooperative project by representatives from the Taiyuan Municipal Optical Fiber Plant and MPT's Houma Cable Plant on the Chinese side and Sumitomo Electric Industries, Inc., on the Japanese side. An optical fiber production line with an annual capacity of 500,000 kilometers [of fiber] will be built in the Taiyuan Municipal High and New Technology Development Zone. Total investment for this project is 210 million yuan RMB. Completion of a 200,000-kilometer-per-year optical fiber production line is planned for the first half of 1994, with completion of the entire 500,000-kilometer-per-year facility by 1998.

Fiber Optic Communications Briefs

Guangzhou-Hong Kong DS5 System Operational

93P60116A Beijing DIANXIN JISHU [TELECOMMUNICATIONS TECHNOLOGY] in Chinese No 12, Dec 92 p 8

[Untitled news brief by Gu Mu [0657 2606]]

[Text] The Guangzhou-to-Hong Kong DS5 optical communications system recently became operational. This system's completion provides Hong Kong, Shenzhen, and principal cities in the Zhujiang Delta with same-circuit video imagery, computer consultation, videotex, fax, and other high-speed broadband information transmission. The DS5 fiber optic cable transmission rate is 565 Mbits/s, and involves the most advanced optical communications technology now prevalent worldwide.

Changzhou Cable Plant Begins Production

93P60116B Beijing DIANXIN JISHU [TELECOMMUNICATIONS TECHNOLOGY] in Chinese No 12, Dec 92 p 8

[Untitled news brief by Gu Mu [0657 2606]]

[Text] The Changzhou Municipal Posts & Telecommunications Fiber Optic Cable Plant in Jiangsu Province was recently completed. The 4-64-fiber communications optical cable product manufactured by this plant was a 1992 key S&T development project. The first batches of JYTA 4-fiber and 8-fiber optical cable have been tested in the Jiangsu Province P&T Management Bureau's Communications Measurement Station, where quality was found to meet the advanced level of comparable products produced elsewhere in the nation.

Satellite Station Will Be First of Its Kind

401000046 Beijing CHINA DAILY in English 28 Dec 92 p 3

[Article by Xie Liangjun]

[Text] Construction of China's first communications satellite control station for civilian purposes got underway on Friday.

The new station, which involves a total 118 million yuan ($20.7 million) in investment, is being built in Northwest Beijing.

One key project for the station will be the Dongfanghong No. 3 communication satellite, which is scheduled for launch at the end of next year.

The station, which is due to go into operation in the first half of 1994, will track, test, control and monitor operation and transmission quality of this satellite.

The station, covering a 3.2-hectare area of land, will be expanded later to control and monitor three to four synchronous communication satellites, according to sources within the Ministry of Posts and Telecommunications.

The technically advanced and highly automated station will import major facilities from the United States.

Partial use of the station is expected from October next year [1993].

China Telecommunications Broadcast Satellite Corporation (China-Sat), under the Ministry of Posts and Telecommunications, will be in charge of constructing and managing the station.

The Dongfanghong series of China's satellites concern telecommunications. The Dongfanghong No. 3 satellite will have 24 transponders and can orbit for 7 to 8 years.

END OF FICHE DATE FILMED

12 February 1993